EXPERIMENTAL INVESTIGATION OF HEAT PIPE PERFORMANCE AT DIFFERENT INPUT CONDITIONS

A Thesis
Submitted in partial fulfillment of
requirements for the degree of

Master of Engineering
in
Thermal Engineering

by

Deepinder Singh
Registration No.: 801583008

Under the Supervision of

Mr. Sumeet Sharma
(Associate Professor, M.E.D.)

Dr. D. Gangacharyulu
(Professor, Ch.E.D)

MECHANICAL ENGINEERING DEPARTMENT

THAPAR UNIVERSITY, PATIALA

June, 2017

Certification

This is to certify that the thesis entitled "**EXPERIMENTAL INVESTIGATION OF HEAT PIPE PERFORMANCE AT DIFFERENT INPUT CONDITIONS**" submitted by **DEEPINDER SINGH** in fulfilment of the requirements for the award of the degree of **Master of Engineering** in **Thermal Engineering** at **Thapar University, Patiala** is a bonafide record of research work carried out by him under our supervision and guidance. No part of the matter embodied in this report has been submitted to any other university or institute for the award of any degree.

(Sumeet Sharma)
Mechanical Engineering Department
Thapar University, Patiala – 147004

(D. Gangacharyulu)
Department of Chemical Engineering
Thapar University, Patiala - 147004

21/6/2017

Declaration

I, **DEEPINDER SINGH,** hereby declare that the thesis, entitled **"EXPERIMENTAL INVESTIGATION OF HEAT PIPE PERFORMANCE AT DIFFERENT INPUT CONDITIONS"**, submitted to **Mechanical Engineering Department, Thapar University** in partial fulfillment of the requirements for the award of the degree of **Master of Engineering** in **Thermal Engineering** is a record of original and independent research work done by me during the period 2015–2017, under the supervision and guidance of **Mr. Sumeet Sharma**, Associate Professor, Mechanical Engineering Department and **Dr. D. Gangacharyulu**, Professor, Department of Chemical Engineering, Thapar University. The work contained in this thesis has not been previously submitted to meet the requirements for a degree or diploma at this or any other higher education institution.

Deepinder Singh

(Deepinder Singh)

Regd. No. 801583008

Dedicated to my parents

Acknowledgements

I would like to express my deep gratitude to Mr. Sumeet Sharma and Dr. D. Gangacharyulu for their invaluable suggestions, excellent supervision, constant encouragement, thought provoking discussions and unabashed inspiration in nurturing the work and during the preparation of manuscript throughout the research work.

I am also thankful to Mass International, Ambala Cantonment, India for helping me in constructing the experimental setup and allowing me an access to their experimental and calibration facilities. This research work carried out by me involves frequent visits to their workshop to get practical exposure in the field of my research.

I also express my indebtedness to my family for their infinite support at each and every part of my life.

Deepinder Singh.

(Deepinder Singh)

Abstract

Heat pipes are known as superconductors of heat because of their fantastic heat transfer and heat extraction ability with minimum heat loss. A lot of research and experimentation has been carried out on heat pipes in the 21st century due to modernization and miniaturization of equipments. Gravitational and capillary forces play a very important role in deciding the overall performance of a heat pipe. At every different inclination, the resultant of these two forces varies, so the performance of a heat pipe also changes. So there is a need to study the performance of heat pipe at different tilt angles.

This study demonstrates the effects of different heat loads on the thermal conductivity of a copper-water heat pipe. The results are presented through experimental as well as analytical method based on capillary limit of heat pipe, which are found to be in fair agreement with maximum and minimum deviations of 29.89% and 6.87% at 40 W and 100 W respectively. The present study also aims at discovering the tilt angle of the same heat pipe at which least thermal resistance is offered. A performance comparison is hence established among heat pipe inclinations, based on which it is perceived that heat pipe offers lowest thermal resistance of 0.033 ˚C/W at 25˚ tilt angle and 90 W heat input. Many different working fluids can be used inside the heat pipe. In recent times, nanoparticles are also being employed in heat pipes to improve their performance. This research work also includes the comparison in the performance of heat pipe with and without Al_2O_3 nanofluid. It was observed that the addition of nanoparticles inside the base working fluid significantly reduced the thermal resistance of heat pipe compared to the heat pipe operating on pure water working fluid.

Hence, selecting an adequate working fluid according to heat pipe constructional material and wick properties is very necessary. The heat transfer coefficient on the external surface of heat pipe condenser section was determined by experimental method and then predicted by empirical correlations. The results from both the cases were in fair agreement with permissible deviation of ± 25%. This study was performed under free as well as forced convection.

Keywords: Heat pipe; Thermal conductivity; Thermal resistance; Free convection; Tilt angle; Wick structure; Capillary limit.

Table of Contents

List of Figures

List of Tables

Nomenclature

A	Cross-section area, m^2
d	Diameter, m
F	Frictional coefficient, Pa/W-m
g	Acceleration due to gravity, m/s^2
Gr	Grashof number
h	Heat transfer coefficient, W/m^2-K
J	Mechanical heat equivalent, J/cal
k	Thermal conductivity, W/m-K
K	Wick structure permeability
L	Length, m
Nu	Nusselt number
r	Radius, m
Ra	Rayleigh number
Re	Reynolds number
t	Thickness, m
T	Temperature, ^oC
ΔT	Temperature gradient, ^oC
Q	Heat Input, W

Greek Symbols

σ	Surface tension, N/m
θ	Contact angle, degree
μ	Viscosity, $N-s/m^2$
ρ	Density, kg/m^3
λ	Latent heat of vaporization, J/kg
$\in$	Wick porosity

Subscripts

a	Adiabatic
b	Bulk
ah	Axial hydrostatic
c	Condenser
e	Evaporator
hc	Condenser phase change
he	Evaporator phase change
h,v	Vapour hydraulic radius
i	Inner
o	Outer
nh	Normal hydrostatic
pc	Pipe wall condenser
pe	Pipe wall evaporator
pa	Pipe axial
s	Solid
sat	Saturation
T	Transported
v	Vapour
va	Axial vapour flow
w	Wall
wa	Axial wick
wc	Condenser wick
w,c	Condenser side wall
we	Evaporator wick
w,e	Evaporator side wall

Chapter 1

Introduction

1.1 Introduction to the thesis

Evolution of heat, which is sometimes undesired, is a common phenomenon in many industrial and engineering applications. With every passing day, the demands for heat removal and heat recovery systems are increasing due to the advancement in machinery that deals with high heat loads. So there is a demand for a device that is efficient in performance, compact in size, and that can transfer heat over the desired range with minimum temperature differential across its ends, thus reducing the heat load on the concerned equipment. Heat pipe is a mechanical device that can fulfil the above mentioned requirements.

In the traditional heat transfer units of the 1880s like Perkin's boiler, the simplest mechanism of transfer of heat was employed where liquid through the pipes was heated by hot gases passing over them [1]. It was not till 1944 when Gaugler's wick concept of heat transfer – which is the basis of heat pipe, came into play [2]. In the early 1960s, Grover after having followed the works of Gaugler introduced term 'Heat Pipe' for the very first time. It is the highest and most economical heat conductance mechanical unit of heat transfer today [3].

A typical heat pipe mainly consists of 3 sections in a cylindrical container – evaporator section, adiabatic section and condenser section, with a wick material lined on the inner circumference of the container. The wick serves as a path for liquid flow while the inner cavity is where the vapours travel. Initially, the liquid or working fluid in the evaporator section absorbs heat from an external source causing it to evaporate and travel to the condenser – where it emits heat through free or forced convection, hence condensing the vapours into liquid form. The wick structure returns this liquid condensate back into the evaporator by the virtue of capillary forces, which is sometimes assisted by gravity as well. The unique structure and the working capability of heat pipe makes it one of the fastest and most economical units of heat transfer in different applications [4, 5].

Heat pipes are also known as superconductors of heat because of their fantastic heat handling abilities with minimum heat loss. Heat pipe is very similar to a thermosyphon in some aspects. But the key difference is that a heat pipe can also operate against gravitational

forces, while thermosyphon cannot, since it lacks the wick structure and hence cannot provide the driving capillary force that is supposed to get the condensate back into the evaporator section. The container material, the wick material and the working fluid are the 3 important parameters to be considered while designing a heat pipe. They are selected based on the application to be addressed and other compatibility criteria [6]. Figure 1.1 shows the schematic of a conventional heat pipe where the heat input section (evaporator) is marked in red colour and heat rejection section (condenser) is marked in blue colour.

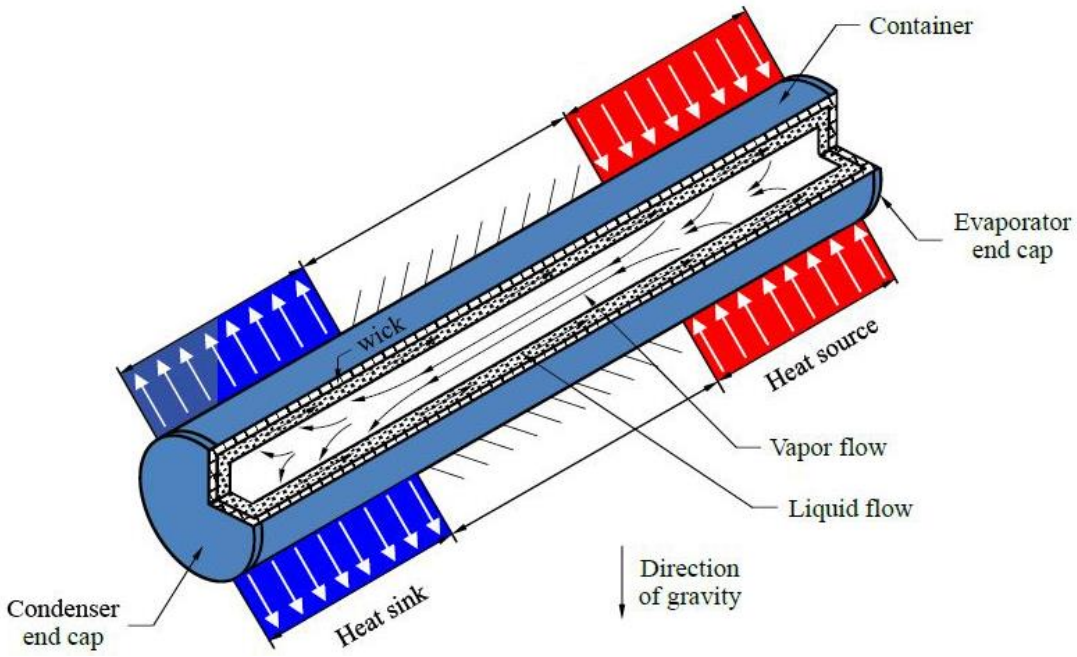

Figure 1.1: Schematic of a conventional cylindrical heat pipe [6].

1.2 Scope of work

All the prime heat transfer parameters like thermal resistance, thermal conductivity and heat transfer coefficient will be evaluated and compared under different heat inputs on the evaporator section of copper-water heat pipe in this study.

Heat pipes have a wide range of applications and they are of a great use in many fields. Since a copper heat pipe is being used in my study, so only the heat loads under 100 W would be considered. To study higher heat load applications, other working fluids may be employed which show a better heat transfer characteristics and can handle higher temperatures. From the past few years, nanofluids are also being used as working fluids which offer great results in their domain of application.

The maximum heat load on a laptop's processor is about 50 W which needs to be dissipated out continuously. Some small capacity computer servers that generate heat within 100 W are also under the scope of my study. Exhaust waste heat generated by most industries carry heat in the range of 20-100 W which should be dissipated out or which could be used to warm up the inlet air that is drawn into the industry by using a connection between inlet duct and exhaust duct with a heat pipe or a set of heat pipes.

By using the results that I gather from my thesis work, I would be able to suggest the inclination at which the copper-water heat pipe should be used to get the best results. And also the heat load that is handled the best according to the heat pipe capabilities can be figured out. By using all these results, the copper-water heat pipe could be utilized in the most effective way in future, hence solving the heat dissipation related problems inside a machine or an industry. It would also be established through this study whether the addition of Al_2O_3 nanofluid in the base working fluid of water is helpful in improving the performance of heat pipes or not.

Chapter 2

Literature Review

2.1 Construction of a heat pipe

The three basic sections in a typical heat pipe are shown in Figure 2.1. A heat pipe generally has the following main constructional features or components [4]:

- The container
- The working fluid
- The wick

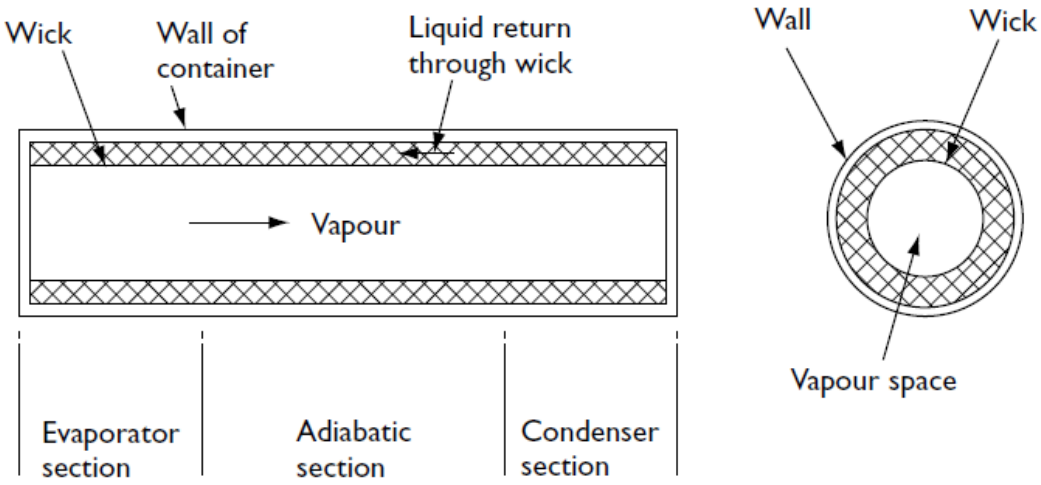

Figure 2.1: The main sections of a typical heat pipe [1]

2.1.1 The container

The heat pipe is built up of a vacuum sealed hollow container or tube which contains all the three necessary sections – evaporator, adiabatic and condenser. The container must be made from a material that has high thermal conductivity, such as copper. At one point of operation, only a small amount of container is filed with liquid working fluid while the rest of it is occupied by vapour state of the same liquid. The wick structure develops necessary capillary forces on the working fluid condensate in the condenser. The container should be chosen in such a way that it has good strength to weight ratio. Sometimes, fins are provided on the condenser end of the container to enhance the heat rejection rate as a result of increase in the surface area [4-6].

2.1.2 The working fluid

It is the fluid that is continuously in the operation inside the working heat pipe. Here are some of the considerations to be kept in mind while selecting a working fluid.

- ✓ Good compatibility with heat pipe wall and wick material
- ✓ High thermal stability and surface tension
- ✓ High latent heat and thermal conductivity

Depending upon the useful working range to be addressed, the working fluids can be chosen from Table 2.1. Sometimes the Merit number is also very useful to compare two different working fluids. Merit number is directly proportional to surface tension, latent heat of vaporisation and liquid density while it is inversely proportional to liquid viscosity. A high Merit number is always desirable for a working fluid [4].

Table 2.1: Selection of working fluids [4]

Medium	**Melting point** (˚C)	**Boiling point** (˚C)	**Useful range** (˚C)
Ammonia	-78	-33	-60 to 100
Pentane	-130	28	-20 to 120
Acetone	-95	57	0 to 120
Methanol	-98	64	10 to 130
Ethanol	-112	78	0 to 130
Heptane	-90	98	0 to 150
Water	0	100	30 to 200
Toluene	-95	110	50 to 200
Mercury	-39	361	250 to 650
Lithium	179	1340	1000 to 1800
Silver	960	2212	1800 to 2300

2.1.3 The wick

The wick structure inside the heat pipe is used to transfer the condensed liquid back to evaporator section. Wrapped screen is the commonly used type of wick structure. The primary role of a wick is that it should produce capillary pressure, and it should pass the liquid back into the evaporator section at the desired rate. Different wick structures offer different magnitude of capillary forces

which play an instrumental role in bringing the fluid back to evaporator from condenser [4, 5]. A lot of research has been done worldwide to investigate the behaviour of different types of wicks so that the wick of best type and material could be suggested based on the requirement. Some of the wick structures commonly employed in heat pipes are shown in Figure 2.2.

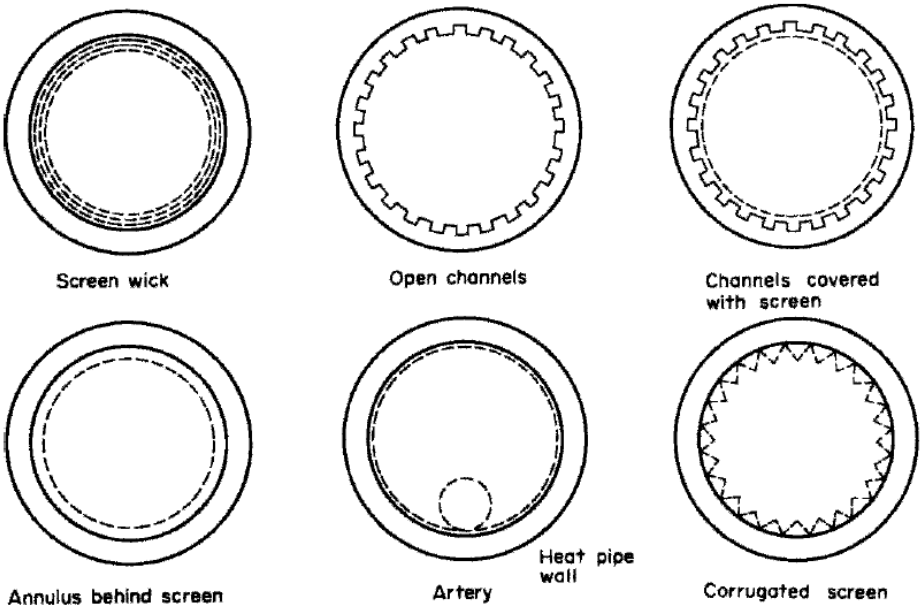

Figure 2.2: Section view of different wick structures [4]

2.2 Working of a heat pipe

A heat pipe works on the basic thermodynamic principles of evaporation and condensation as represented in Figure 2.3. As discussed above, It is a vacuum sealed unit that comprises of evaporator and condenser connected through an adiabatic section. The working fluid saturates the wick pores in such a way that vapour and water lie in an equilibrium state by developing enough vapour pressure at the desired or required temperature range.

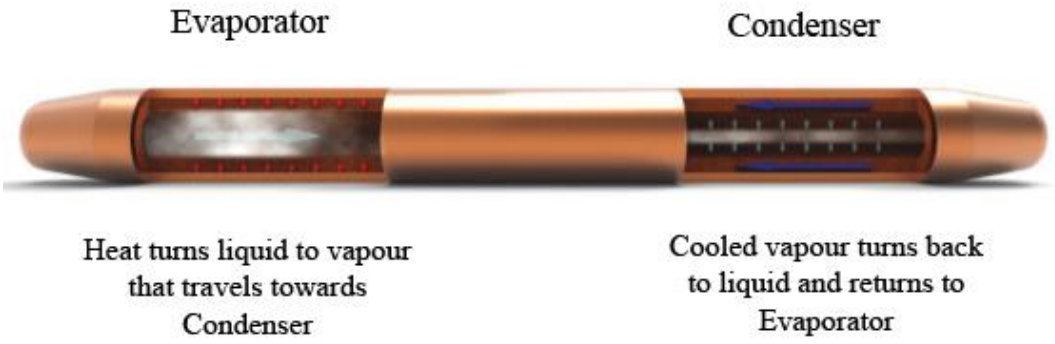

Figure 2.3: Working of a heat pipe [5]

The liquid residing inside the wick is forced to evaporate when heat is applied at the end. This makes the hot vapour diffuse and occupy the central section of the heat pipe as well. Condensation of the vapour happens when the temperature is lower than that of the evaporator, even if it is only by a little amount. The vapours then liberate the heat in the condenser section. Because of the high effective thermal conductance, constant temperatures are maintained across the length of a heat pipe unit. Connecting a heat sink to a part of heat pipe establishes a vapour flow pattern which in turn can make condensation happen at this very point of heat transfer. The cycle is completed when the condensate is returned from the condenser end to the evaporator part by the use of capillary forces. The heat pipe system is well proven in many areas and applications, the most prominent of them are the aerospace applications. It is capable of transferring heat energy at over a hundred times superior rate compared to the solid metallic conductors of same physical dimensions [7].

2.3 Types of heat pipe

Depending on different applications, we employ different heat pipes to serve our purpose. Except the constructional details, the basis of working remains the same in every heat pipe. Besides the widely used and most popular cylindrical heat pipe, some other types of heat pipes are as mentioned below [4-6].

- Changing Conductance Heat Pipes
- Pressure Controlled Heat Pipes
- Oscillating Heat Pipes
- Heat Pipe Heat Exchangers
- U-Tube Heat Pipes
- Thermosyphons
- Rotating Heat Pipes
- Loop Heat Pipes

2.4 Usage limitations in heat pipe

The role of pressure variation along the evaporator and the pressure recovery of inertial pressure is always considered. The prime limitations in using a heat pipe are represented in Figure 2.5 which shows the variation of axial heat flux with temperature. The effects of vapour pressure change due to inertial effects are shown in Figure 2.4. While the inertial

pressure keeps dropping as we move along the evaporator section, all of it is recovered at the end of condenser, though the pressure recovered is significantly lesser according to Cotter's theory.

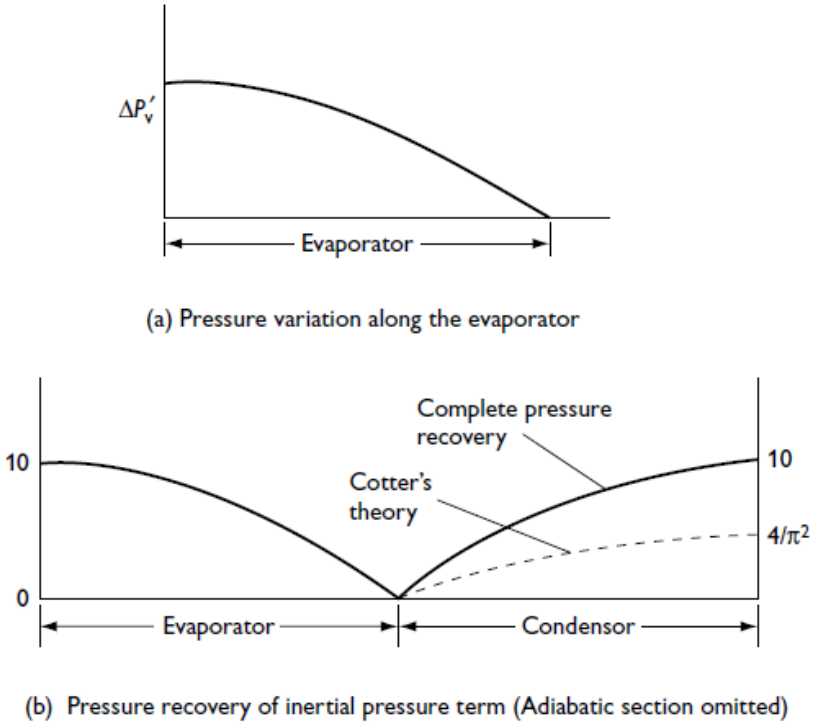

Figure 2.4: Vapour pressure change due to inertial effects [4]

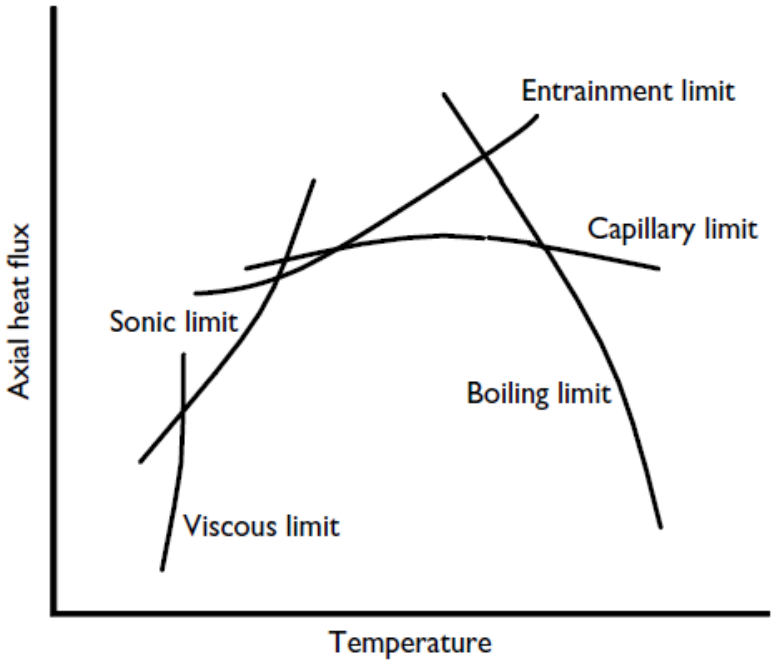

Figure 2.5: Limitations to heat transfer in a heat pipe [4]

The heat pipe has to operate inside the dome region of Figure 2.5 only. In order for the heat pipe to function well, the maximum capillary pumping pressure ($\Delta P_{c,max}$) should always be more than the total pressure drop inside the heat pipe. This pressure drop comprises of 3 components as mentioned below :-

(i) The pressure drop to bring the liquid from condenser back to the evaporator. (ΔP_l)
(ii) The pressure drop so that the vapours from the evaporator can reach the condenser. (ΔP_v)
(iii) The pressure due to gravity which could be zero, positive or negative - which depends on the orientation of the heat pipe. ($\Delta P_g{}^1$)

Equation (2.1) must be kept in mind while designing a heat pipe, It combines all the above mentioned four pressure drop terms into a single equation.

$$\Delta P_{c,max} \geq \Delta P_l + \Delta P_v + \Delta P_g^1 \qquad (2.1)$$

The heat pipe will not be able to work properly if this relation is not satisfied. So it must be taken care of while designing a heat pipe [4, 8].

2.5 Applications of heat pipes

Heat pipes, owing to their exceptional performance, are a good fit for various applications. They can be used for cooling semiconductor elements, transformers, I.C. engines, mobile phones, electric motors, turbine machinery, light water nuclear reactors, etc. Miniaturization and modernization has increased the demand for heat pipes [9-11]. By virtue of its nature, a heat pipe always tries to operate at constant temperature so as to avoid uneven temperature areas across its body. All desktop computers and laptops make use of microprocessors. So heat pipes are used inside them as it allows the computer system to work smoothly by continuously extracting undesired heat out of the system. Old desktop computers employ a finned heat sink in series with the processor which also required a fan for forced convection purpose to remove heat load. It has been replaced with heat pipes in latest computers as they are more reliable and efficient. Heat pipe also eliminates the need of a fan as it can operate under natural convection condition too, thus reducing the noise that could have otherwise resulted from a forced convection fan. However, to achieve a higher external surface value of heat transfer coefficient, a forced convection mechanism can be used on the condenser side of the heat pipe. High heat loads on modern day servers can also be handled easily by heat pipes. In general, the applications of heat pipes are broadly classified into following groups.

2.5.1 Separation between sink and source

A heat pipe can be used to transfer heat to long distance range as well, because of its high thermal conductivity. In some cases where part cooling is needed as shown in Figure 2.6, it is useless to scatter the heat using a heat sink placed immediately next to that part. So a certain separation or gap is necessary in such cases.

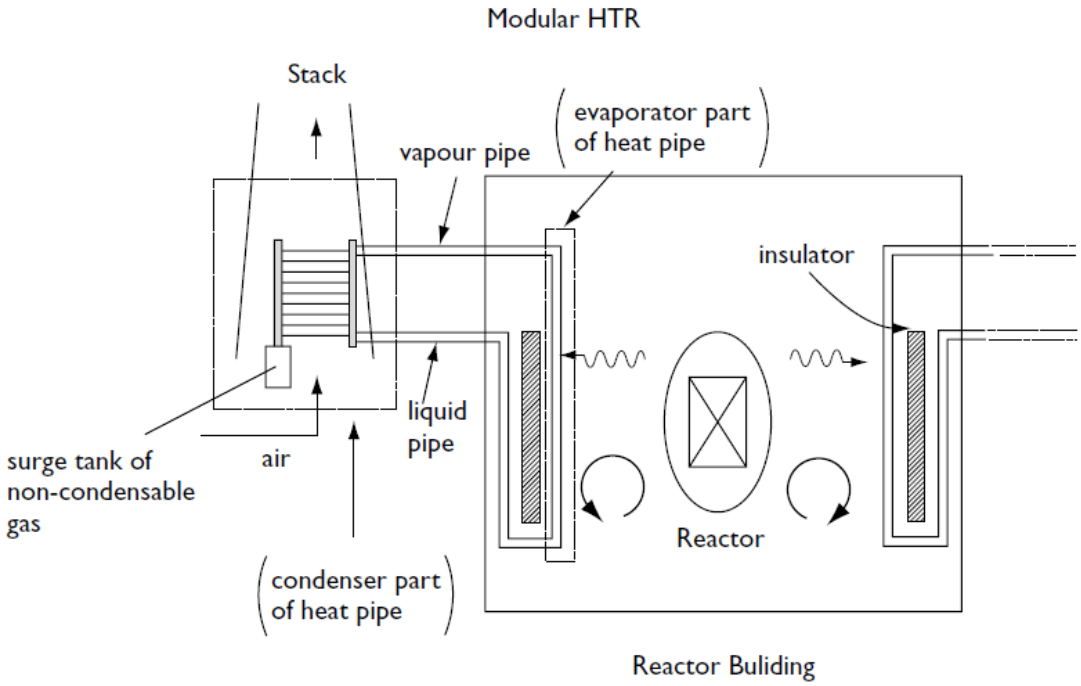

Figure 2.6: Heat removal from high temperature reactor through heat pipe [4]

2.5.2 Flattening of temperature

This property is almost similar to the first application. By virtue of its nature, a heat pipe always tries to operate at constant temperature so as to avoid uneven temperature areas across the body of pipe. Sometimes the evaporator part could be facing the Sun while the condenser could be in shade. Heat pipes are now designed to operate under different external conditions smoothly. Even in space programs, use of heat pipes has been proposed and introduced [12].

2.5.3 Transformation of heat input

Heat flux basically deals with the heat input per unit area of the evaporator. Many reactor technologies and machines use transformation of heat flux input. In the branch of Thermionics, the transformation of low heat flux into high heat flux and vice versa is achieved easily [12].

2.5.4 Temperature control

As the name clearly suggests, we use a variable conductance heat pipe to perform the duty of temperature control. The temperature of devices installed over the evaporator section could be controlled as per the need using this heat pipe. VCHP is used extensively in furnace or ovens but its most important application is its use in aircrafts and planes [12].

2.5.5 Heat diodes

Thermal diode is of a great use in the cases where we need the transfer of heat to happen in one particular direction only. A heat pipe has to satisfy a number of things or conditions to be finally considered as acceptable for various industrial applications. Any equipment has to be of long lasting span, safe and easy to work with, Heat Pipe is no different in that respect [12].

2.6 Previous research work in heat pipe field

Zhang et al. [13] studied about the implementation of heat pipe in industrial applications and other equipment in China where two main subjects in this field were presented – Technology extension and Research. A lot of experimental as well as theoretical research was carried out on two phase flow behaviour and science related to heat pipe, which decided the applications for which heat pipes could be used. Some special cases of industrial applications involving industrial process equipment and waste heat recovery mechanisms were introduced. In some boilers and air preheaters, carbon steel-water heat pipes have been successfully implemented which helped in recovering waste heat, thus protecting environment and conserving energy. The technology of heat pipes was also used in ammonia convertors and other chemical reactors.

Loh et al. [14] compared the heat pipe performances in various inclinations. The Author started every experiment at +90˚ vertical position where condenser blocks were at the top of evaporator blocks. The test was conducted in a 180° sweep that stopped at the inclination angles of +60˚, +30˚, 0˚ (horizontal), -30˚, -60˚ and –90˚. Initially, heat load of 10 Watt and 5 Watts was applied to the evaporator blocks. The power supply was increased as per the programs instructions in the steps of 5 Watts when the test at every orientation angle came to a steady state at a specified time period. It was concluded that for 6 mm outer diameter, the groove heat pipe gives significantly better thermal output compared to mesh or sintered

powder metal heat pipe in the horizontal 0˚ to vertical +90˚ range. Also it was established that the heat source inclination and gravity have less effect on heat pipe of sintered powder metal. It should be kept in mind not to use mesh or groove heat pipes in the situations where the evaporator's position is on the top of condenser.

Kang et al. [15] performed an experiment in which the action of silver nanofluid on performance of heat pipe was investigated. The Author used this nanofluid as the working medium inside a deep grooved circular heat pipe of 211μm width × 217μm depth. Temperature distribution was measured through this experiment and comparison was done on the heat pipe performance using nanofluid and deionized water. The nanoparticle concentrations under test were in the range 1 mg/l to 100 mg/l. The condenser side was cooled by a 40 ˚C water bath in which constant temperature was maintained. At a same charge volume, the nanofluid filled heat pipe temperature distribution showed that the thermal resistance decreased in the range of 10% to 80% compared to deionized water at input power range between 30W to 60 W. The results hence gathered also proved that the thermal resistances of the heat pipe significantly reduced with an increase in size and concentration of silver nanoparticles.

Noie et al. [16] investigated the thermal performance of a thermosyphon under ordinary functioning conditions at various inclination angles. A number of experiments were performed at tilt angles varying from 5˚ – 90˚ and evaporator filling ratios varying from 15% – 30%. A thermosyphon made out of copper material having outside diameter, inside diameter and lengths of 16mm, 14.5mm and 1000mm respectively was used in the study. The working fluid inside the container was distilled water. According to the results observed by author, the best thermal performance was seen in the tilt angle range of 15˚to 60˚. A genuine agreement was found between author's results and previous literature results. Lastly, the maximum condensation heat transfer coefficient corresponding to filling ratios 22% and 30% was seen at 30˚ and for filling ratio 15%, it was seen at 45˚.

Meena et al. [17] used check valve operated closed loop oscillating heat pipes (CLHOP-CV) made up of copper tubes with R123 as working fluid to study the effect of different tilt angles and internal diameters. The fliing ratio inside the evaporator section was fixed at 50% and lengths of all three sections of heat pipe were same. Tilt angles were varied from 0˚ to 90˚. The adiabatic section of heat pipe was insulated, also a cold water bath was employed in this

study to continuously extract heat out of condenser end. In the results, it was seen that heat pipe's critical temperature increased as the internal diameter was changed from 1.77 mm to 2.03 mm or when the tilt angle was increased from 0˚ to 90˚.

Huddakorn et al. [18] studied the effects of oscillating heat pipe orientation on its overall performance. The heat pipe under investigation was made up of Pyrex glass tube having inner width and evaporator span of 1mm and 50mm respectively. The number of meandering turns were taken as ten. All 3 sections of the heat pipe were of same length. The working fluid with filling ratio 50% was R123. It was observed from the results that at horizontal position of the heat pipe, insufficient condensed liquid film resulted in dry-out of evaporator. When the tilt angle was increased from horizontal position all the way up to vertical position, performance limit arose due to evaporator section flooding. The author then performed a second set of experiment known as quantitative study where oscillating heat pipes were made up of copper tubes instead of Pyrex glass, with inner diameters of 0.66 mm, 1.06 mm and 2.03 mm respectively. The meandering turns were kept same but 3 different lengths of evaporator section were employed, i.e. 50 mm, 100 mm and 150 mm. R123, ethanol and water were taken as working fluids with same filling ratio as in first set of experiment. It was found in the results that for all different inclination angles, critical heat flux was inversely proportional to evaporator length, and directly proportional to internal diameter of heat pipe.

Huminic et al. [19] performed a computational fluid dynamics study of heat pipes operating on water-nanofluid (copper-oxide) working fluid by using the three fluid governing equations – continuity, momentum and energy to increase the thermal performance of heat pipe. Three different volume fractions were used in the study – 0%, 1% and 4% and the analysis was done in laminar, adiabatic and steady state conditions with multiphase flow at P_{sat} 0.12335 bar and T_{sat} 325.15 K. The incompressible steady flow was studied in various regions of the heat pipe. The fluid flow was modelled using ANSYS CFX and ACAD 2002 was used to draw geometry. In the boundary conditions, positive and negative heat fluxes were given at evaporator and condenser respectively. The fact that nanofluids possess higher convection heat transfer coefficient and critical heat flux compared to water was the reason why the heat pipe performance was significantly enhanced.

Grooten et al. [20] used very large length-to-diameter ratio thermsyphons with R-134a as working fluids to perform his experiments to analyse the effects of saturation temperature,

inclination angle, filling ratio on the limiting operational heat flux. It was observed that the thermosyphon functions effectively under inclination angles of 83˚. The filling ratio of heat pipe wasn't critical over the values of 25%. It was also observed that when the saturation temperature was increased, or when the inclination angle was decreased – the operation limiting heat flux reduced. Inclination angles more than 83˚ were not recommended by the author for the heat pipe to work properly.

Teng et al. [21] presented the study of enhancement of thermal efficiency of heat pipe charged with nanofluid. He considered alumina nanofluid which was produced by direct synthesis method with three different concentration (0.5, 1.0 and 3.0 wt. %). The nanofluid was dispersed many times with the help of ultrasonic vibrator and electromagnetic agitator and suspension was statically placed for 1 month to ensure good suspension. He took a straight copper pipe with 8 mm inner diameter and 600 mm length and investigated the effect of different charged amount and tilt angle. His investigation revealed that performance of heat pipe was optimized at 1.0 wt. % concentration of nanofluid and increased efficiency of 16.8% compared to the base fluid.

Riehl et al. [22] studied water-copper nanofluid application in an open loop pulsating heat pipe. They used an open loop pulsating heat pipe with water-copper nanofluid by using an addition of 5% by mass of copper nanoparticles. Improvements on the overall device's operation were noticed by the author when using the nanofluid with lower temperatures. In their work, more bubbles were formed, so more intense pulsations were observed during the PHP operation, which resulted in more presence of vapour in the channels. Hence higher thermal conductances were seen when compared to the pulsating heat pipe operation with pure water as the working fluid.

Mousa [23] studied the effect of nanofluid concentration on the performance of a heat pipe. Author used pure water and Al_2O_3-water based nanofluid as working fluids. An experimental setup was made to study the heat pipe performance in varying operating conditions. The effect of fraction of nanoparticles in base fluid by volume, filling ratio, and the input heat flux on the thermal resistance of the heat pipe was studied. Total thermal resistance of the heat pipe for pure water and Al_2O_3-water based nanofluid was also predicted. The Author

observed that the thermal resistance decreases with increasing Al_2O_3-water based nanofluid compared to that of pure water.

Senthilkumar et al. [24] studied the behaviour of heat pipe operated on aqueous solutions of n-Pentanol at various orientations. Research objective was to do a comparison test between heat pipe working with water and n-Pentanol as working fluids at different inclination angles. The results drawn out from this study showed superior performance of the heat pipe when working on n-Pentanol fluid because of the simple reason that the aqueous solutions have a positive gradient of surface tension with respect to temperature. Using water as working fluid has some disadvantages, even though it is the most widely used working fluid. In order to remove those limitations, the working fluid water can be substituted with a dilute aqueous solution of n-Pentanol. The biggest advantage of using n-Pentanol is that it has very high capillary limit and boiling limit, thus it makes a heat pipe suitable for large heat load applications.

Kumar et al. [25] studied the heat transfer inside a heat pipe by comparing an analytical model with experimental data. In his work, the evaporator part of heat pipe is under forced convective heating and condenser part is under free convective air cooling. A theoretical analytical model was developed based on the thermal resistance network approach. The model that was developed determined thermal resistances, not just at outer surface of the evaporator and condenser, but also in the interior part of the heat pipe. A test setup was developed to find the thermal performance of the heat pipe. The effects of various operating parameters, like heat pipe inclination angle and heating fluid temperature at evaporator inlet, were experimentally studied. The experimental results hence obtained were used to compare the results from analytical model. The heat transfer coefficients predicted by the model at the outer surface of the heat pipe were observed to be in a decent agreement with experimental results. The maximum heat transport rate of the heat pipe was achieved at a tilt angle of 25◦ at 70◦C heating fluid temperature.

Solomon et al. [26] carried out experiment to study the effect of coated wick on the performance of heat pipe by taking wick of screen type (100 mesh/inch) with and without deposition of the nanoparticles.80-90nm copper nanoparticle were coated over the wick surface by simple immersion technique and followed by drying and heat pipe was tested at

three different heat flux. The result showed that with coated heat pipe wall temperature decreases as compared to uncoated heat pipe further it revealed that thermal resistance of the evaporator section decreased and that of condenser increased but overall thermal resistance was lower than that of conventional and it decreases with increased heat input. He observed 40% reduction in thermal resistance and 40% increase in the heat transfer coefficient.

Moraveji et al. [27] investigated the thermal performance of heat pipe by taking aluminum oxide nanoparticle of diameter 35nm. He took a heat pipe made of copper with different length which has sintered wick structure and 90˚ curve between the evaporator and condenser section. Tested concentrations of nanofluids were 0%, 1% and 3% by weight. He compared the result obtained with heat pipe charged with pure water. His results showed that increase in heat input increases the wall temperature, the wall temperature of the heat pipe with nanofluid was less as compared to the heat pipe charged with the pure water also wall temperature decreased with higher nanoparticle concentration also with increased nanoparticle concentration, the temperature difference decreases. Result indicted that the thermal resistance of heat pipe with nanofluid was lower than that of water heat pipe.

Manimaran et al. [28] discussed the factors affecting thermal performance of heat pipes in their review paper. This paper offered a review about various parameters due to which operation of circular heat pipes is affected. It also throws light on how the selection of a working fluid, orientation, filling ratio, input load, etc can affect the thermal resistance and thermal conductance of a heat pipe. It was shown through results that the heat transfer was enhanced when the filing ratio was in the range of 40% - 85%. It was suggested by the Author to operate the heat pipe in carefully chosen orientation so as to achieve better performance.

Pachghare et al. [29] used Akachi's patented closed loop pulsating heat pipe with 10 turns of copper tubes to experimentally study the effects of its inclination angle on thermal performance. The inner diameter of heat pipe was 2 mm while its outer diameter was 3.6mm. The lengths of 3 sections of heat pipe was same, i.e. 50 mm while its filling ratio was 50%. Water, methanol and R-134a were employed as working fluids inside heat pipe. It was later found that R-134a's performance was the best compared to other 2. The heat input over evaporator section was increased from 5 W to 50 W with increments of 5 W at different inclination angles. According to the results obtained by the author, as the heat input was

increased, the thermal resistance of heat pipe was reduced. The performance was found to be more sensitive under the heat loads of 25 W compared to heat loads above 25 W. Due to the gravitational forces, it was seen that vertical bottom heat pipe position gave best thermal performance at all inclinations.

Hung et al. [30] carried out their investigation with alumina nanofluid which was produced by direct-synthesis using dispersant cation chitosan as base fluid. He took three variants of the nanofluid 0.5, 1.0 and 3.0 by wt. % in the heat pipe, a straight copper tube having 9.52 mm outer diameter and different lengths of the heat pipe (0.3 m, 0.45 m and 0.6 m) different charged volume ratio of base fluid 20%, 40%, 60%, 80%, respectively, effect of tilt angle 10˚, 40˚, 70˚ and 90˚, different heat input (20 W, 30 W and 40 W) and studied the effect of these variants on the effective thermal conductivity of the heat pipe in order to know thermal performance of heat pipe. Result demonstrated that every parameter affected the performance of the heat pipe.

Peyghambarzadeh et al. [31] worked on thermal performance of different working fluids in a dual diameter circular heat pipe. The performance of a circular heat pipe of 40 cm length was experimentally checked. Basically, the heat pipe had two diameters, broader in evaporator and narrower in adiabatic and condenser regions. Three different working fluids – water, methanol and ethanol were introduced separately inside the heat pipe. Evaporator is subjected to low heat flux values. While in condenser, the Author used a constant temperature water bath at 15 ˚C, 25 ˚C, and 35 ˚C. Compared to methanol, results obtained showed that higher heat transfer coefficients were obtained for water and ethanol. Also with increase in heat flux, the heat transfer coefficient at evaporator rises. Using methanol, reduction in heat transfer coefficient is observed at high heat fluxes which are probably due to the surface dryout effect. Increasing the orientation decreased the heat pipe thermal resistance.

Xue et al. [32] performed experiments to study the performance of a pulsating closed loop heat pipe with 50% filling ratio ammonia working fluid. The heat pipe was made out of quartz glass with six turns. The inner and outer diameters were 2 mm and 6 mm, respectively. The circulation of flow could be seen by visual investigation only, but the author had to perform 4 case tests to determine the effects of heat pipe orientations on its performance. The results showed that, at any random inclination angle, the ammonia circulation was very smooth and easy. Thermal resistance as low as 0.02 K/W was achieved which reflects on the

efficient and fast performance of heat pipe. Also thermal resistance was found to be inversely proportional to inclination angle. The ammonia CLPHP at horizontal 0° position when subjected to low input load was very easy to start-up, but the flow of working fluid is such case was slow.

Idrus et al. [33] studied the thermal performance of a cylindrical copper heat pipe with sintered powder wick and having an outer diameter of 10 mm and length 300 mm at different heat inputs and inclination angles. The thermal performance of heat pipe was decided on the basis of temperature differential between evaporator and condenser sections, which helped out in calculating the thermal resistance and thermal conductivity. The best results were obtained when the inclination angle of heat pipe was between 30˚ and 60˚ and heat input was between 70 – 80 W.

Kumar et al. [34] carried out the experiment to study the effect of alumina nanoparticle with deionized water base as fluid on heat transfer performance of a copper heat pipe. He studied how filling ratio, tilt angle and heat input affect heat transfer and tested the heat pipe with different filling ratio, tilt angle and heat input and gave the following outcome:

1. Increase in the heat input caused increase in the gradient along the axis of heat pipe and temperature difference between two sections also increased.
2. Thermal resistance decreased due to increase in the inclination angle and acquired the minimum value in vertical position with 80% filling ratio.
3. Operating at 80% filling ratio and 30° inclination angle the optimum efficiency value was achieved.

Yang et al. [35] did a fabrication and performance evaluation of flexible heat pipes for potential thermal control of foldable electronics. Author used a fluoro-rubber tube that acts as a connecting link between the evaporator and condenser sections. Also a strong base treated hydrophilic copper mesh was used as a wick structure. Deionized water in 3 different filling ratios of 10%, 20% and 30% was used as a working fluid so that its effect on the thermal performance on the system could be studied. It was noticed that the fabricated heat pipes could be bended quite easily to the maximum limit of 180˚ horizontally and they produced low thermal resistances despite undergoing bending over and over again. Obviously, the thermal resistance kept increasing with larger bending angles because bending interrupts

normal vapour flow and it also gives rise to increased liquid–vapour interfacial thermal resistance in the evaporator region.

Nazarimenaesh et al. [36] studied the effects of inclination angle, evaporator heat load and condenser side cooling fluid temperature on the performance of a U-shaped sintered heat pipe with each section length of 135 mm. The diameter of heat pipe throughout its cross-section was taken as 6 mm. Ethanol and deionized water were taken as base fluids in which equal amount of silver nanofluid with concentration of 10, 50 and 1000 ppm were added. The range of evaporator side heat input was from 10 W to 40 W and temperature of cooling fluid was taken in the range of 20 to 40 ˚C. It was observed that with the increase in concentration of nanofluids, the thermal resistance of heat pipe was decreased significantly. Also at every tilt angle, overall heat transfer coefficient of the heat pipe was found to be increased. At the inclination angle of 30˚, author achieved lowest thermal resistance for silver nanofluid with 50 ppm. Capillary and gravitational affect the performance of a heat pipe at inclined conditions. At +90˚ these two forces act in the same direction while at -90˚ they act in opposite direction. The author reported least thermal resistance was found at the angle of +90˚.

Hassan et al. [37] studied the effect of alumina nanoparticle prepared by two-step method on the performance of heat pipe taking the nanofluid (1 and 3% wt.) of 20-50 nm diameter size in deionized water and compared the result with heat pipe having deionized water only. For this they took a heat pipe of 10 mm inner diameter, 200 mm brass tube with 50 mm long evaporator and 50 mm long condenser and showed that with nanofluid wall temperature was reduced and the difference between the condenser temperature and evaporator temperature was also reduced. Further he said that the increase in the thermal diffusivity of the nanofluid was 10%. His investigation revealed the variation of viscosity of nanofluid as compared to deionized water and also showed that the evaporator temperature was lesser than that of deionized water with increasing heat input.

Nookaraju et al. [38] performed an experimental and numerical analysis using ANSYS 15 to check the thermal performance of heat pipes. The sintered copper wick heat pipe performed well owing to its brilliant capillarity property while thermosyphon had very low efficiency which resulted from the high temperature differential across the ends of heat pipe.

Hassan et al. [39] studied the effect of deposition of nanoparticle on the porosity of wick after repetitive use of heat pipe. He considered alumina nanoparticle (1, 2 and 3 vol %), filled it in an evacuated copper tube with porous wick and equipped the setup with temperature and vacuum pressure sensor. Experiment revealed that initially heat pipe showed good performance due to the use of nanoparticles but later on performance of heat pipe depreciated due to repetitive use and questioned the suspension stability of the nanoparticle in the base fluid because of the phase change of the base fluid. After repetitive use of heat pipe Images were taken by scan electron microscope for the wick of heat pipe revealed the deposition of aggregated nanoparticle on the surface of the wick. This creates capillary resistance and thermal resistance and depreciates heat pipe performance.

Ghanbarpour et al. [40] studied the effect of increasing and then decreasing heat input on the performance of heat pipe. He considered a copper heat pipe with 6.35 mm outer diameter and 200 mm length having screen mesh wick structure and alumina nanoparticle with different mass concentration of 5% and 10%. The result showed that with 5% concentration heat pipe performance was improved with variable heat input while using 10% concentration performance of heat pipe was deteriorated.

Hong et al. [41] performed a multiple orientations research on heat transfer performances of Ultra-Thin Loop Heat Pipes with different evaporator structures where he developed two Ultra-Thin Loop Heat Pipe prototypes with parallelogram and trapezoidal evaporator configurations for battery thermal management system. As per the results, both the ULHP prototypes displayed good performances despite low assistance from force of gravity, proving that they could easily work in different orientations. The parallelogram configuration curbed the flow instability quite well and hence it showed better behaviour in nullifying the effect of gravity. But there was a certain angle below which these heat pipes didn't perform.

Hussain et al. [42] studied the performance of a heat pipe by simulating it numerically. By using COMSOL Multiphysics package, a numerical model was formed. The absolute thermal resistance of the heat pipe was calculated by following a single phase steady state approach, which gave the top wall temperature profile. The results showed that when the porosity of wick was increased – the conductivity of liquid wick region went down, hence leading to the increase in thermal resistance. Highest thermal resistance was observed when the lengths of evaporator and condenser section were equal. While low values of thermal resistance were

found at large internal radius, because it resulted in more cross section area for heat transfer to take place. The author suggested that better and more accurate results would be obtained when two phase flow modelling is done instead of single phase.

Remeli et al. [43] did an investigation of combined heat recovery and power generation using a heat pipe, the experimental setup of which is shown in Figure 2.7. Industrial waste is recovered and converted into electricity by using a Thermo Electric Generator. Authors designed and fabricated a lab scale bench-top prototype of waste heat recovery. The first heat pipe was connected to the hot side of the TEG and the second to the cold side of TEG. Heat transfer rate, heat exchanger effectiveness, and maximum output power are the parameters in terms of which system performance was studied. TEG showed low efficiency of conversion so its power generation capabilities were not that good. But the system is still pretty useful because the input energy coming into the system would have otherwise been wasted. More development on this could be done in future as suggested by the author himself.

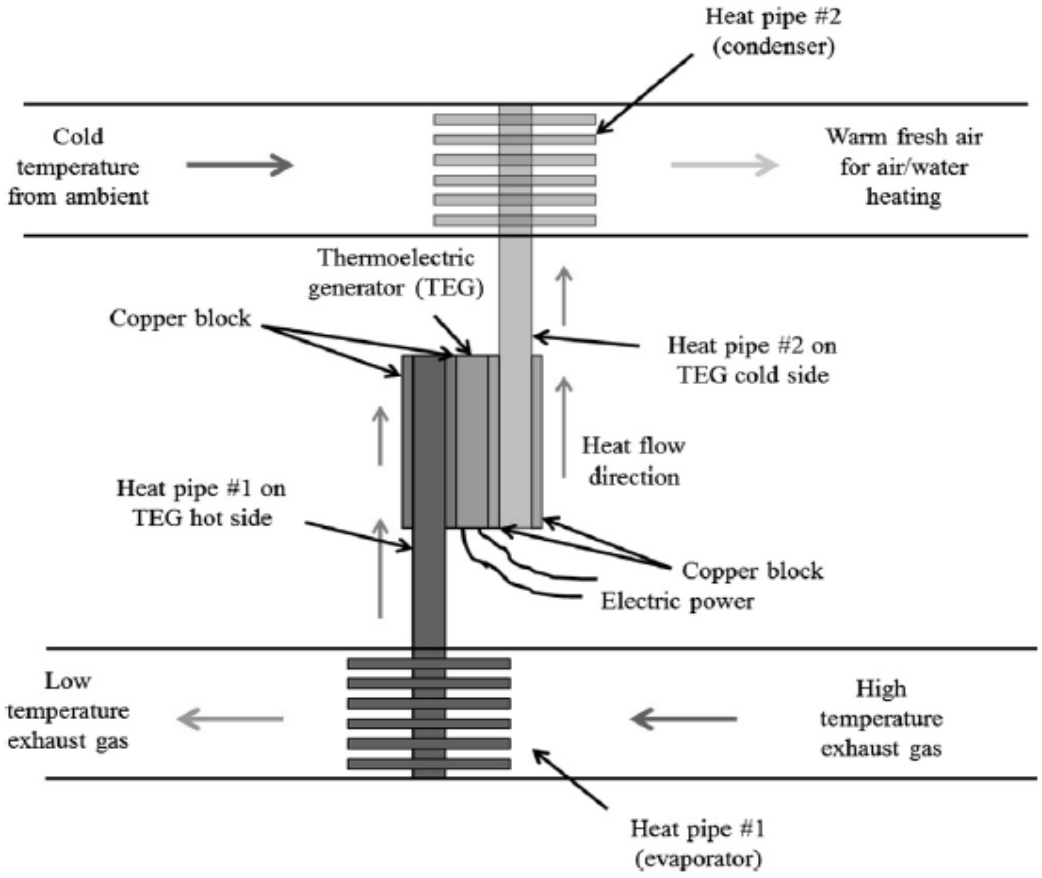

Figure 2.7: Heat recovery system working [43]

Solomon et al. [44] proposed an analytical expression based on the heat transport limitation equations for predicting the thermal conductivity of the heat pipe where author exploited the fact that the heat transfer limit primarily depends on the capillary pumping pressure that the wick generates, pressure losses and some frictional losses. Hence a way of judging the thermal conductivity was found purely on the basis of thermos-physical properties of working fluid and the wick. A good agreement was found when the experimental and analytical results of thermal conductivity of heat pipe were compared. The author also followed lumped resistance method to find effective thermal conductivity. In all three cases, the thermal conductivity was found directly proportional to heat input.

Bhullar et al. [45] studied temporal deterioration in the performance of heat pipe operated on surfactant free aqueous nanofluids. Better and more consistent results were observed at higher heat inputs compared to lower ones. Also the use of nanoparticles increased boiling limit and reduced contact angle which was beneficial.

Cong et al. [46] studied the effects of inclination angle on sintered heat pipe radiator. The results indicated that the inclination angle of heat pipe affects the performance of both evaporator as well as condenser sections. The heat pipe performance was more sensitive in case of negative inclinations compared to positive angle inclinations. The change in thermal resistance of heat pipe was insignificant at low heat loads. When the heat input over heat pipe was 138.46 W at 60˚ tilt angle, the heat pipe thermal resistance was found to be reduced by 82.86% in comparison to horizontal 0˚ position. The author recommended to use the heat pipe radiator in a positive inclination angle such that condenser is above evaporator section. Tilt angles from 30˚ to 90˚ showed best results.

Hong et al. [47] performed a multiple orientations research on heat transfer performances of Ultra-Thin Loop Heat Pipes with different evaporator structures where he developed two Ultra-Thin Loop Heat Pipe prototypes with parallelogram and trapezoidal evaporator configurations for battery thermal management system in year 2016. As per the results, both the ULHP prototypes displayed good performances despite low assistance from force of gravity, proving that they could easily work in different orientations. The parallelogram configuration curbed the flow instability quite well and hence it showed better behavior in nullifying the effect of gravity.

Goshayeshi et al. [48] experimentally studied the effect of tilt angle on heat transfer enhancement of a ferrofluid in a closed loop oscillating heat pipe subjected to magnetic flied. Iron-oxide/kerosene nanofluid was used as working fluid in this study. The range of inclination angles of heat pipe was varied from 0˚ to 90˚ and the heat load on evaporator section was varied from 10 W to 90 W. The heat transfer coefficient was determined with and without the effect of magnetic field. In the results it was seen that heat transfer coefficient increased at higher inclination angles. The critical tilt angle (also the best angle in terms of efficiency and performance) was found to be 75˚. The performance of heat pipe significantly reduced beyond the angle 75˚ because of higher rate of condensed liquid return. Also, when the heat pipe ferrofluid was subjected to magnetic field, the vapour temperature difference between evaporator and condenser section reduced.

2.7 Summary and research gaps identified

The performance of a heat pipe does not just depend on its inclination or tilt angle, but also on its container material, wick structure, working fluid, filling ratio and other properties. Vertical position of heat pipe is not recommended as it results in flooding of evaporator section due to increased speed of condenser return. But heat pipes of generally all types, perform better at inclined conditions compared to horizontal or vertical operation. Addition of n-Pentanol or nanoparticles in the working fluid can also significantly improve the performance of heat pipes.

It was observed that very little research work has been done on the effective thermal conductivity of heat pipe. The percentage in reduction of thermal resistance of the heat pipe on using nonofluids as working fluids as compared to pure water was not clearly established in literature. The enhancement in the heat transfer coefficient over condenser section when the heat pipe is subjected to forced convection instead of natural convection was also not found in literature. All these factors were crucial in deciding the objectives of the thesis.

2.8 Thesis objectives

The following objectives were decided after thorough reading of heat pipe literature in various journals, books and theses.

1. To design heat pipe test rig with provision to adjust the heat pipe at different tilt angles with respect to the horizontal.

2. To find and compare the effective thermal conductivity of the heat pipe in horizontal position at different input loads by experimental method, analytical model and lumped resistance network.
3. To study the performance of heat pipe at different tilt angles by finding its thermal resistance.
4. To compare the performance of heat pipe with and without the use of nanoparticles in the working fluid and to find the percentage reduction (if any) in thermal resistance due to addition of nanoparticles.
5. To predict the condenser side heat transfer coefficient of the heat pipe and compare it with experimental values for free convection as well as forced convection over condenser section.

Chapter 3

Experimental Setup & Methodology

In this chapter, all the details about the experimental setup and the steps followed in the experimental procedure are discussed. The analytical and theoretical backgrounds behind various equations used in the study are also presented in this chapter.

3.1 Details of heat pipe and experimental test rig

The experimental setup primarily involves a heat pipe, procured from M/s. Golden Star, Pune, India along with a heating element, a water tank, a pump, a bypass valve, a rotameter, PT100 resistance temperature detector sensors and a data logging system. PID (Proportional Integral Derivative) mechanism is used to control the water temperature inside the tank. The outer diameter, inner diameter and the axial length of the straight copper water heat pipe under study is 7.8 mm, 6 mm and 180 mm, respectively. A phosphor-bronze square patterned plain wrap wire mesh structure is used inside it.

The provision of a tilting mechanism is provided at the end of the heat pipe evaporator section to give inclinations to the heat pipe assembly to carry out the experiments at different tilt angles by elevating the condenser section while keeping the tip of evaporator section at the same point. A nut and bolt arrangement is used at the evaporator end of heat pipe that can be loosened to change the tilt angle and it can then be tightened to fix the heat pipe at required inclination. A calibrated angular protector is used to change and measure the tilt angles accurately. The lengths of evaporator section, adiabatic section and condenser section are taken as 60 mm, 55 mm and 65 mm, respectively, as shown in Figure 3.1.

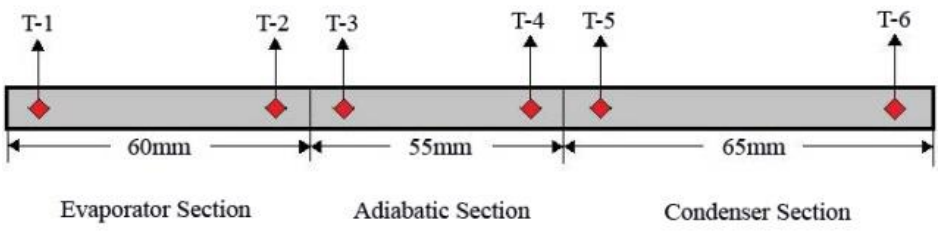

Figure 3.1: Heat pipe section-wise details with thermocouple positions

The RTD sensors are connected to the heat pipe in such a way that it leaves a length of 5 mm from the position of thermocouple to the end of the section, which means that from the leading edge of the heat pipe, the placement of six temperature sensors are at the distances of 5 mm, 55 mm, 65 mm, 110 mm, 120 mm and 175 mm. The adiabatic section of the heat pipe is insulated by using layers of glass wool and polyurethane. This is done so that no heat is able to escape these sections and the heat is rejected from condenser surface only. The heat pipe works as a diode and lengths of its 3 sections can be decided according to experimental requirement. The schematic of heat pipe experimental setup is shown in Figure 3.2 and the details of various instrument used in the setup are given in Table 3.1.

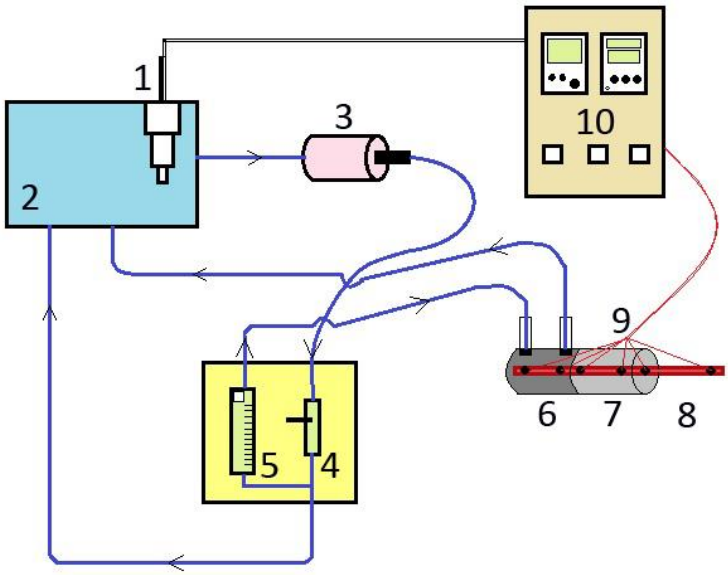

Figure 3.2: Schematic of heat pipe test rig used in the study

Table 3.1: Part description of experimental test rig

1	Heating element
2	Water tank
3	Pump
4	By-pass valve
5	Flow meter
6	Evaporator section of heat pipe
7	Adiabatic section of heat pipe
8	Condenser section of heat pipe
9	Pt-100 RTD sensors
10	Data logger

Table 3.2: Some equipments used with their specifications

S.No.	Equipment	Application	Make	Specification
1.	Temperature data logger	Records and displays the temperature	i-therm AI-5441	Resolution 1˚C Accuracy 0.3% FS 90 - 270 VAC/DC
			i-therm AI-7481	
2.	Rotameter	Flow measurement of hot water	Flowstar FSA-100	10-200 ml/min
3.	Centrifugal pump	Circulation of hot water	Vijay-50 Monobloc Pump	Head 15 m Capacity 240 LPH Drive 0.05 KW 230 VAC/DC
4.	Temperature sensors	Measuring heat pipe surface temperatures	Mass International	Accuracy ± 1˚C Range -100 to +250˚C

The equipment details relating to the experimental test setup are as given in Table 3.2. Out of these instruments, the rotameter and temperature sensors were calibrated before using them in the actual experimental work. Calibration is necessary as it helps us to determine the accuracy of the instrument.

The temperature to which the water is required to be heated in the tank can be set at the start of the experiment by giving the input to the heating element. A PID controlling mechanism is used for the same purpose which calculates and minimises the error between set value and process value. The desired heat input to the evaporator of heat pipe in Watts can be controlled either by changing the temperature of the water or by changing the mass flow rate of water that enters the evaporator section. However, for the sake of calculation and simplicity, the mass flow rate in the experiments is kept constant at 100 ml/min and only the temperature values are changed while performing experiments at different heat inputs.

After achieving the desired steady state temperature, the pump is turned on which transports the heated water from the tank towards the heat pipe evaporator jacket. In this process, the water also passes through a bypass valve where the excess water is released back into the tank and the remaining water is allowed to enter the rotameter to measure the flow rate. In this way the input load is given to the evaporator section of the heat pipe. The water

outlet is also provided at the end of evaporator section which releases the water in the evaporator jacket back to the tank after heating has been done. The front view of fabricated heat pipe experimental setup used in the study is shown in Figure 3.3.

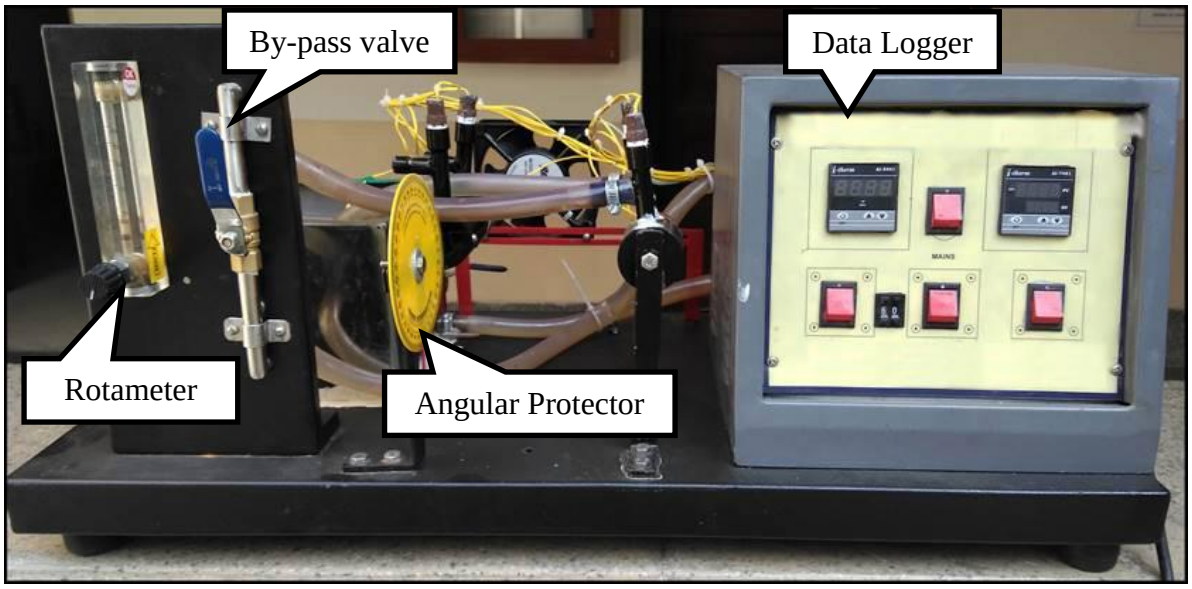

Figure 3.3: Heat pipe experimental setup

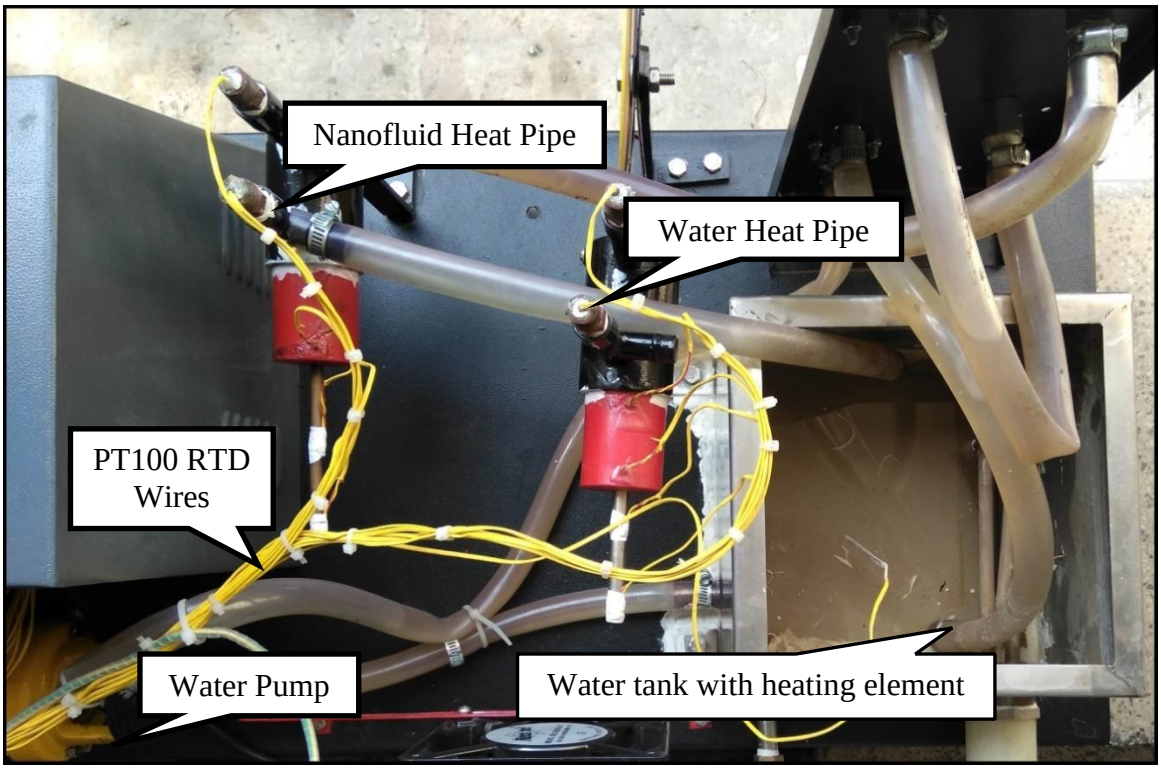

Figure 3.4: Top view of heat pipe experimental setup

The assembly of heat pipe experimental setup can be better understood from the top view of test rig as shown in Figure 3.4. It shows the passage and piping structure of water from the tank to the heat pipe evaporator section after passing through flow control valve and rotameter. The evaporator section jacket is painted with black colour, adiabatic section jacket with red colour while the condenser section of the heat pipe is open to the surroundings.

3.1.1 Calibration of rotameter

The flow measuring device, rotameter was calibrated before performing experimental work. A stop watch and a transparent measuring beaker was used for that purpose. Flow rate on rotameter was fixed at different rates and the water was collected in a beaker after passing through rotameter.

A stopwatch was used to find the time in which the water level in the beaker reaches the value set in rotameter. The calibration was performed in five sets at six different flow rates, i.e. 25 ml/min, 50 ml/min, 75 ml/min, 100 ml/min, 125 ml/min and 150 ml/min. The calibration readings are provided in annexure Table A1 and rotameter calibration graph is shown in Figure 3.5.

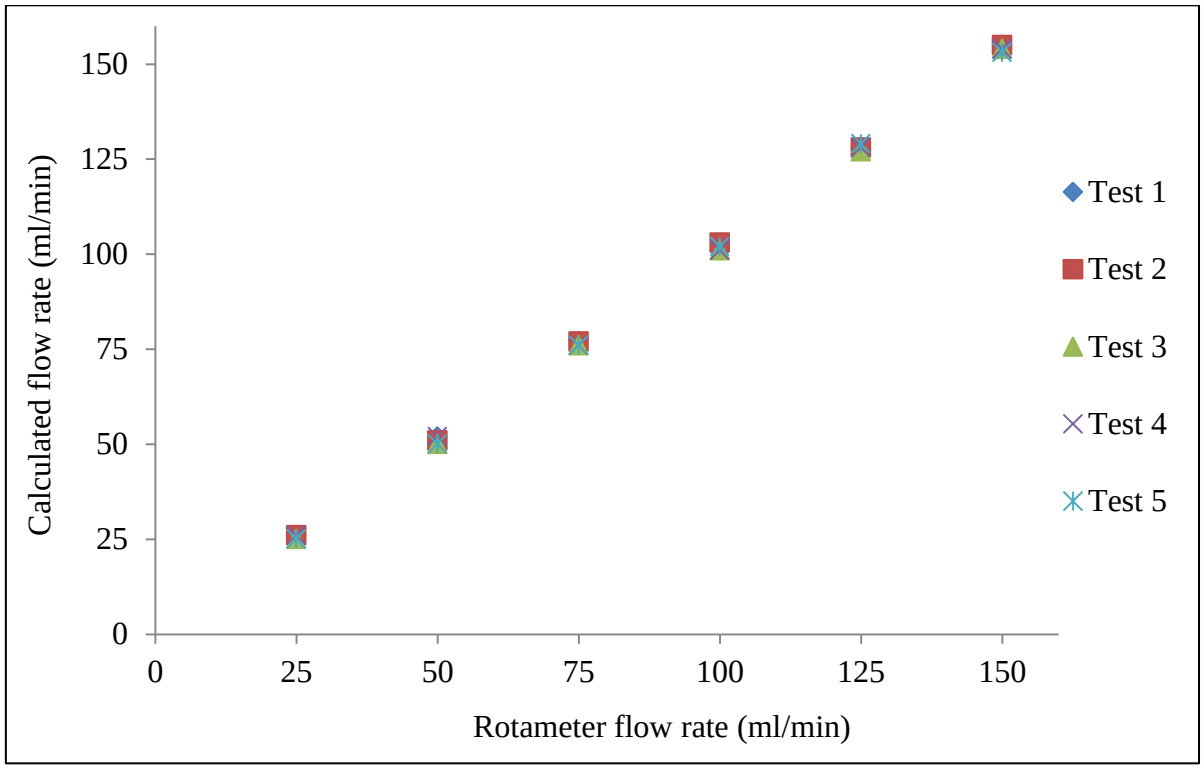

Figure 3.5: Rotameter calibration graph

3.1.2 Calibration of temperature sensors

A total of 12 temperature sensors are used in this study over two different heat pipes. Each heat pipe contains 6 RTD sensors. RTD stands for resistance temperature detector. The RTDs are made up of pure materails, generally nickle, copper or platinum. The sensors used in this research work are made of platinum, hence they are reffered to as PT100 RTDs. They have a resistance of 100 ohms at zero degree centigrade. Before performing experiments, these temperature sensors were calibrated and their accuracy was determined. A standard thermometer and a water bath was used to perform the calibrations.

All the sensors were connected to temperature display system and inserted inside a water bath along with the thermometer. The temperature of the water bath was increased in gradual steps to do the calibration at different temperatures. Readings were taken and compared at 8 different tempratures, i.e. 20 ˚C, 25 ˚C, 30 ˚C, 35 ˚C, 40 ˚C, 45 ˚C, 50 ˚C, 55 ˚C and 60 ˚C.

Deviation found between temperature sensor reading and thermometer reading was found to be ±1 ˚C to 1.5 ˚C. The calibration readings are provided in annexure Tables A2 and A3. The calibration graphs of RTDs over water and nanofluid heat pipe respectively are given in Figure 3.6 and 3.7, respectively.

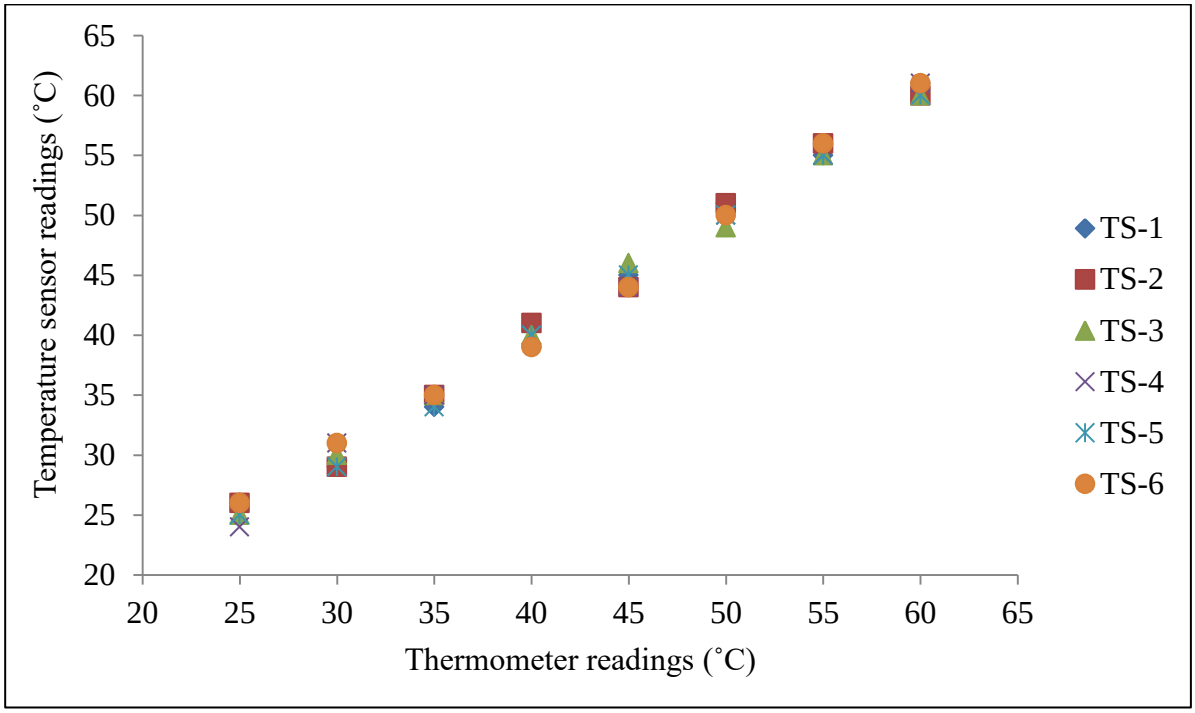

Figure 3.6: Calibration graph of temperature sensors used on water heat pipe

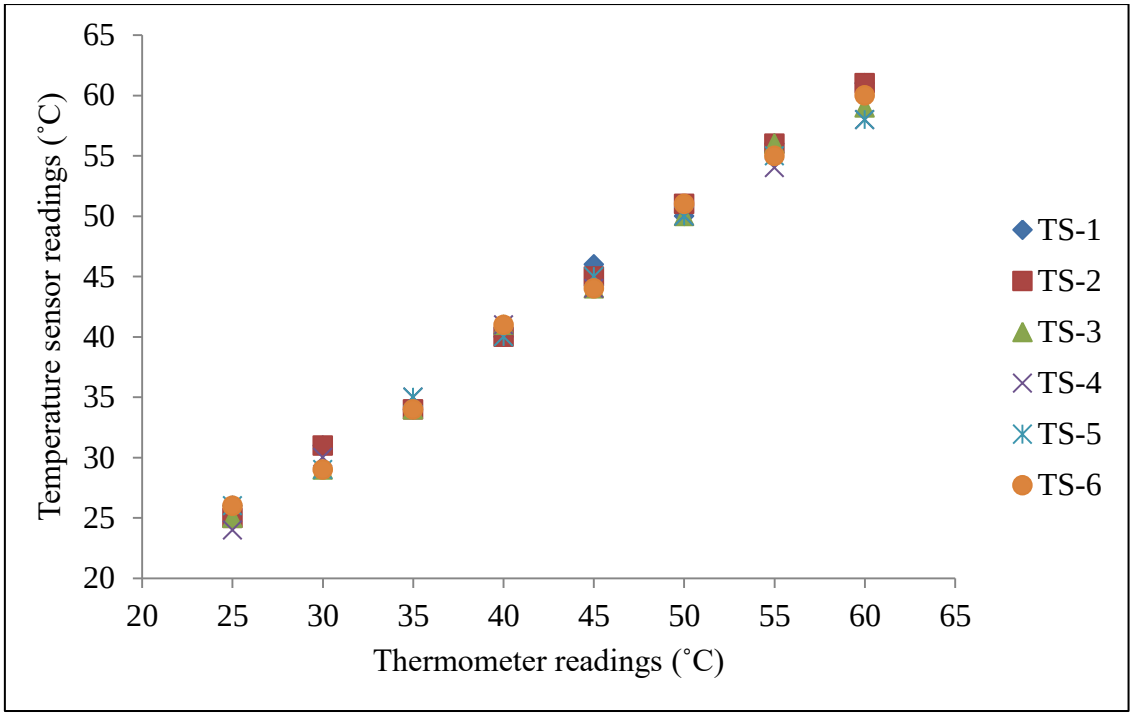

Figure 3.7: Calibration graph of temperature sensors used on nanofluid heat pipe

From the calibration results of rotameter and temperature sensors, it was established that the instruments are accurate enough and efficient to be used for experimental work. The various dimensions and specifications of the copper-water heat pipe used in the study are as shown in Table 3.3.

Table 3.3: Heat pipe specifications and their notations

S.no	**Notation**	**Parameter**	**Value**
1.	A_v	Vapour core region cross-section area	1.9625×10^{-5} m
2.	A_w	Wick cross-section area	8.635×10^{-6} m^2
3.	d_v	Vapour core diameter	5×10^{-3} m
4.	k_s	Thermal conductivity of solid wick material	50 $W m^{-1}k^{-1}$
5.	k_p	Thermal conductivity of heat pipe material	400 $Wm^{-1}k^{-1}$
6.	k_{wick}	Effective thermal conductivity of wick	1 $Wm^{-1}k^{-1}$
7.	L_e	Evaporator section length	60×10^{-3} m
8.	L_a	Adiabatic section length	55×10^{-3} m
9.	L_c	Condenser section length	65×10^{-3} m
10.	r_i	Inside radius of heat pipe	3×10^{-3} m
11.	r_o	Outside radius of heat pipe	3.9×10^{-3} m
12.	$r_{h,v}$	Hydraulic radius of heat pipe	2.5×10^{-3} m
13.	t_p	Heat pipe wall thickness	0.9×10^{-3} m
14.	t_w	Wick wire thickness	0.0406×10^{-3} m

3.2 Experimental method to find thermal conductivity

With the assumption that the heat gained by the heat pipe is equal to heat transported by the heat pipe, Fourier heat conduction principle can be used to find the experimental thermal conductivity of heat pipe as given by the following equation [44].

$$k_{exp} = Q\frac{L_{eff}}{A\Delta T} \tag{3.1}$$

Where Q is the rate of heat transfer, A is pipe cross-section area, ΔT is temperature differential from evaporator to condenser section and L_{eff} is effective length of heat pipe which is calculated by Eq. (3.2)

$$L_{eff} = \left(\frac{L_e + L_c}{2}\right) + L_a \tag{3.2}$$

Where L_e, L_a and L_c denotes the lengths of evaporator, adiabatic and condenser sections of heat pipe respectively.

3.3 Analytical expression for thermal conductivity

Based on the thermo-physical properties of water, wick and geometric information about the heat pipe, an equation can be developed to predict the effective thermal conductivity of the heat pipe. Capillary force generated in the wick is one of the most important factors that decide the heat transport limit inside the heat pipe, which is why it forms the basis of this analytical calculation. Some other limitations are entrainment limit, boiling limit, viscous limit and sonic limit. For the sake of simplicity, heat conducted by the heat pipe is assumed equal to the heat transport limit. As discussed in Chapter 2, the heat pipe will work spontaneously and efficiently only if the net capillary pumping pressure between condenser and evaporator is more than the sum of all pressure losses that happen in the two-phased flow inside the heat pipe. If this requirement is not met, it may lead to unwanted phenomenon of condenser blockage or evaporator dry-out. Knowing that the capillary pressure must be more than or equal to other pressure losses, the following equation can be considered [44]-

$$\Delta P_c = \Delta P_v + \Delta P_l + \Delta P_{he} + \Delta P_{hc} + \Delta P_{nh} + \Delta P_{ah} \tag{3.3}$$

Where,

ΔP_c = maximum capillary pressure generated

ΔP_v = vapour phase inertial and viscous pressure drop

ΔP_l = liquid phase inertial and viscous pressure drop

ΔP_{he} = evaporator phase change pressure drop

ΔP_{hc} = condenser phase change pressure drop

ΔP_{nh} = normal hydrostatic pressure drop

ΔP_{ah} = axial hydrostatic pressure drop

Inertial effects and transition losses in vapour phase are neglected and only viscous effects are considered. It is also assumed that along the axial direction within the heat pipe, vapour flow is one-dimensional. With these assumptions, Eq. (3.3) is reduced to Eq. (3.4).

$$\frac{2\sigma Cos\theta}{r_c} = \frac{16\mu_v L_{eff} Q_T}{2r_{h,v}^2 A_v \rho_v h_{fg}} + \frac{\mu_l L_{eff} Q_T}{K A_w \rho_l h_{fg}} + \rho_l g d_v \qquad (3.4)$$

Where,

θ = contact angle

μ_v = vapour viscosity at different temperatures (N-s m^{-2})

μ_l = liquid viscosity at different temperatures (N-s m^{-2})

Q_T = capillary limit of heat pipe (W)

$r_{h,v}$ = hydraulic radius of heat pipe (m)

A_v = vapour core region cross-section area (m)

A_w = wick cross-section area (m^2)

ρ_v = vapour density at different temperatures (kg m^{-3})

ρ_l = liquid density at different temperatures (kg m^{-3})

h_{fg} = heat of vaporisation at different temperatures (J kg^{-1})

g = acceleration due to gravity (m s^{-2})

d_v = vapour core diameter (m)

From equation (4), we can find the value of Q_T as represented in Eq. (3.5)

$$Q_T = k_{eff} A \frac{\Delta T}{L_{eff}} = \left(\frac{2\sigma Cos\theta}{r_c} - \rho_l g d_v\right)\left[\frac{16\mu_v L_{eff} Q_T}{2r_{h,v}^2 A_v \rho_v h_{fg}} + \frac{\mu_l L_{eff} Q_T}{K A_w \rho_l h_{fg}}\right]^{-1} \qquad (3.5)$$

Where, K is wick structure permeability which can be obtained by Eq. (3.6)

$$K = \frac{d_w^2\, \varepsilon^3}{122(1-\varepsilon)^2} \qquad (3.6)$$

Where, d_w is wick structure diameter, which is 6mm and ε is wick porosity which is 0.7363.

The final expression for predicting thermal conductivity of the heat pipe can be obtained on rearranging the Eq. (3.5), where A is cross-section area of heat pipe (4.7×10^{-5} m^2) and ΔT is average temperature differential across the heat pipe, which will be different for different heat load experiments. Hence, the analytical expression for effective thermal conductivity is finally obtained as shown in following equation [44].

$$k_{eff} = \frac{h_{fg}\left(\frac{2\sigma Cos\theta}{r_c} - \rho_l g d_v\right)}{A\Delta T\left[\frac{16\mu_v}{2r_{h,v}^2 A_v \rho_v} + \frac{\mu_l}{K A_w \rho_l}\right]} \tag{3.7}$$

3.4 Lumped thermal resistance network approach

The different thermal resistance components in the heat pipe are as shown in Figure 3.8.

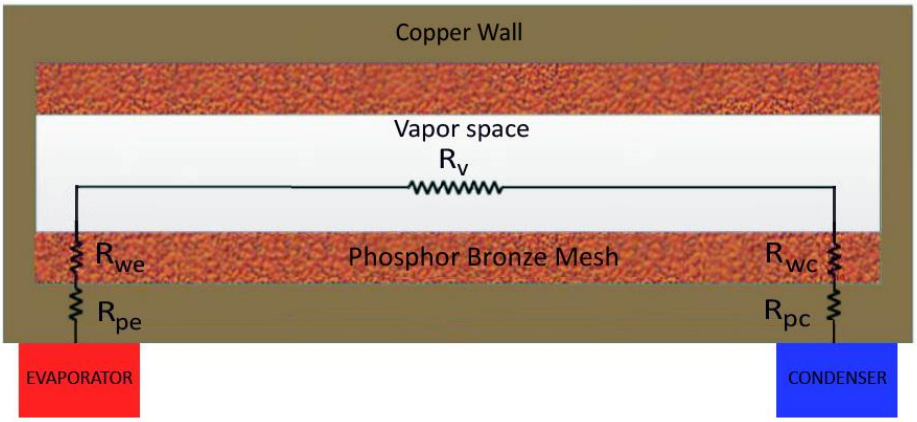

Figure 3.8: Lumped thermal resistance network

The expression for overall thermal resistance of the heat pipe is given by the following equation [5].

$$\frac{1}{R_{total}} = \frac{1}{R_{pe} + R_{we} + \frac{1}{\frac{1}{R_{va}} + \frac{1}{R_{pa}} + \frac{1}{R_{wa}}} + R_{wc} + R_{pc}} \tag{3.8}$$

Where,

R_{total} = total thermal resistance of heat pipe.

R_{pe} = thermal resistance offered by heat pipe wall in evaporator section.

R_{we} = thermal resistance offered by wick in evaporator section.

R_{va} = thermal resistance due to vapour flow in heat pipe.

R_{pa} = axial thermal resistance offered by pipe wall.

R_{wa} = axial thermal resistance due to wick.

R_{wc} = thermal resistance offered by wick in condenser section.

R_{pc} = thermal resistance offered by heat pipe wall in condenser section.

As per the literature, there are a number of correlations and formulas to find the magnitude of different components that offer resistance to the flow of heat in the heat pipes. Eq. (3.9) to (3.13) can be used to find the individual resistance components. They are known as Chi correlations [49].

$$R_{pe} = \frac{r_o t_p}{2L_e k_p} \tag{3.9}$$

$$R_{we} = \frac{r_o^2 t_w}{2L_e r_i k_{wick}} \tag{3.10}$$

$$R_v = \frac{\pi r_o^2 F_v \left(\frac{L_e}{6} + L_a + \frac{L_c}{6}\right) T_{v,e}}{\rho_v \lambda J} \tag{3.11}$$

$$R_{wc} = \frac{r_o^2 t_w}{2L_c r_i k_{wick}} \tag{3.12}$$

$$R_{pc} = \frac{r_o t_p}{2L_c k_p} \tag{3.13}$$

Where,

r_o = outside radius of heat pipe, m

t_p = heat pipe wall thickness, m

L_e = evaporator section length, m

L_a = adiabatic section length, m

L_c = condenser section length, m

k_p = thermal conductivity of heat pipe material (copper), W/m-K

t_w = wick wire thickness, m

r_i = inside radius of heat pipe, m

k_{wick} = effective thermal conductivity of wick, W/m-K

F_v = frictional vapour coefficient, Pa/W-m

$T_{v,e}$ = vapour temperature at evaporator, ˚C

ρ_v = fluid vapour density, kg/m^3

λ = latent heat of vaporization, J/kg

J = mechanical heat equivalent, J/cal

$$F_v = \frac{(f_v Re_v)\gamma_v}{2A_v r_{h,v}^2 \lambda} \tag{3.14}$$

$$k_{wick} = k_f \left[\frac{(k_f + k_s) - (1-\epsilon)(k_f - k_s)}{(k_f + k_s) + (1-\epsilon)(k_f - k_s)}\right] \tag{3.15}$$

$f_v Re_v$ = drag coefficient

γ_v = kinematic viscosity, m^2/s

A_v = vapour core area, m^2

$r_{h,v}$ = vapour hydraulic radius, m

k_f = thermal conductivity of fluid, W/m-K

k_s = thermal conductivity of solid wick material, W/m-K

ϵ = volumetric porosity of wire mesh

Based on the above equations and details, effective thermal conductivity of the heat pipe can be obtained by using the following equation [44].

$$k_{eff} = \frac{L_{eff}}{R_{total}} \tag{3.16}$$

From the resistance network Eq. (3.8), it is clear that all the axial thermal resistance components can be neglected because of the fact that the value of R_{va} is very small. Now, having known the thermal conductivities at different temperatures by experimental method, the results could be verified and compared with the analytical methods by using the correlations and equations discussed above. The calculations to be done for sections 3.3 and 3.4 are only for copper-water heat pipe. So the effect of nanoparticles can be neglected in that case. All the properties used are of water only, as it is the only working fluid inside the heat pipe. However, in the subsequent section, a heat pipe using nanoparticles is brought into picture too, so that their performance with and without nanofluids can be compared.

3.5 Heat pipe inclination study and effect of nanofluid

Experiments are performed at heat pipe tilt angles of 0˚, 5˚, 10˚, 15˚, 20˚, 25˚, 30˚, 35˚, 40˚ and 45˚ with respect to the horizontal to check the thermal performance of the heat pipe by finding its thermal resistance by using the following equation [24].

$$R = \frac{\Delta T}{Q} \tag{3.17}$$

Where ΔT is the temperature difference between evaporator and condenser sides while Q is the input heat at the evaporator end in Watt. The values of thermal resistance can hence be obtained at different heat inputs corresponding to different orientation positions of heat pipe. The angle that offers least thermal resistance can be determined based on this study. The wick structure/material and the capillary pressure generated by it is the most important parameter that influences the thermal resistance behaviour of the heat pipe. Different wicks used in the same heat pipe under same conditions will show different thermal performance behaviour of the heat pipe.

A comparison was also done in the thermal performance of heat pipe with water as a working fluid and a heat pipe with Al_2O_3 nanoparticles dispersed in water as working fluid. Alumina nanoparticles are likely to reduce the thermal resistance of the heat pipe and consequently increase its effective thermal conductivity because coating of nanoparticles on the mesh structure reduces the contact angle and increases the boiling limit of the heat pipe. The wick material and structure used in both the heat pipes in this thesis work is same. Research has been done over the past few years by using various working fluids out of which nanofluids are one of the types. The dispersion of these tiny nanoparticles inside the working fluid increases the heat transport characteristics of base fluids along which they are used. Hence there are a lot of advantages of using nanofluid based heat pipes. However, the choice of using nonofluids inside heat pipe is also considered controversial by a few researchers as they have often encountered the problem of agglomeration and sedimentation of the nanoparticles in the mesh structure which results in poor performance of the heat pipe with the passage of time.

3.6 Condenser side heat transfer coefficient

In this section, the empirical correlations to predict the heat transfer coefficient on the external condenser surface of heat pipe are given for free and forced convection.

3.6.1 Heat transfer coefficient for free convection

Firstly, the thermophysical properties of air are obtained at film temperature, T_f (which is the average of wall temperature of heat pipe and the ambient temperature). For seven different set of experiments at different loads, the film temperatures and the corresponding values of air properties are as given in annexure Table A4. Grashof number, Gr, is calculated by using the following equation [50].

$$Gr = \frac{g\beta(T_c - T_a)L^3}{\nu^2} \tag{3.18}$$

The Rayleigh number, Ra can be obtained by multiplying Grashof number and Prandtl number. If the value of Ra exceeds 10^9, then the flow is turbulent. Otherwise the flow is considered laminar. Churchill and Chu proposed some empirical relations to calculate Nusselt number, Nu, for flat plate. If $10^{-1} < Ra < 10^{12}$, then Nusselt number is given by Eq. (3.19) and if $0 < Ra < 10^9$, then Nusselt number is given by Eq. (3.20)

$$Nu_{plate} = \left\{ 0.825 + \frac{0.387\, Ra^{\frac{1}{6}}}{\left[1 + \left(\frac{0.492}{Pr}\right)^{\frac{9}{16}}\right]^{\frac{8}{27}}} \right\}^2 \tag{3.19}$$

$$Nu_{plate} = 0.68 + \frac{0.670\, Ra^{1/4}}{\left[1 + \left(\frac{0.492}{Pr}\right)^{9/16}\right]^{4/9}} \tag{3.20}$$

The Nusselt number given by Eq. (3.19) and Eq. (3.20) is for flat plate but the heat pipe under study is cylindrical. So these empirical relations can be corrected by using Eq. (3.21)

$$Nu_{corrected} = Nu_{plate}(1 + 1.43\xi^{0.9}) \tag{3.21}$$

Where,

$$\xi = \left(\frac{L}{d_o}\right) Gr^{-1/4} \tag{3.22}$$

The heat transfer coefficient on the outside condenser surface of heat pipe can then be predicted by using Eq. (3.23). The predicted heat transfer coefficient can be compared to experimental value to find the percentage deviation and accuracy of the model [50, 51].

$$h = \frac{Nu\, k_{air}}{L} \tag{3.23}$$

3.6.2 Heat transfer coefficient for forced convection

We can also determine the heat transfer coefficient by subjecting the condenser end of heat pipe to cross flow forced convection using a fan and duct. Hence we can make a comparison between free and forced convection and determine the enhancement in heat transfer. Temperature measuring device is required at the inlet and outlet part of the duct to determine mean bulk temperature, T_b which represents energy or temperature average inside the duct. The total heat transfer in this case can be expressed by using the following equation [51].

$$Q = hA(T_w - T_b) \tag{3.24}$$

Here, T_w denotes the wall temperature of the heat pipe. The most common correlation to predict the Nusselt number in the case of forced convective turbulent flow is given by Dittus and Boelter which is as give in Eq. (3.25). This correlation is only applicable for fully developed turbulent flow in smooth tubes.

$$Nu = 0.023 Re^{0.8} Pr^{n} \tag{3.25}$$

Since the fluid is being heated in this case, so the value of 'n' is considered as 0.4, but in case of cooling, it is taken as 0.3. Large errors can arise on using Dittus and Boelter correlation which can be reduced to as low as 10% by using Gnielinski correlation which is valid over large range of Reynolds number. Hence we can obtain more accurate results for Nusselt number in forced convection by using Eq. (3.26) because it also incorporates friction factor, which can be determined from Moody diagram. In case of smooth tubes, the friction factor is calculated using Eq. (3.27).

$$Nu = \frac{\frac{f}{8}(Re - 100)Pr}{1 + 12.7\left(\frac{f}{8}\right)^{2}(Pr^{\frac{2}{3}} - 1)} \tag{3.26}$$

Where,

$$f = (0.790 \ln Re - 1.64)^{-2} \quad (3.27)$$

The Gnielinski correlation is valid when Prandtl number lies in the range 0.5 to 2000 and Reynolds number lies in the range 3000 to 5×10^6. Due to uncertainties and assumptions present in empirical formulas, deviations might be seen between experimental and predicted results.

3.7 Summary

The details about heat pipe and the experimental setup are given in this chapter. The experimental formulas and empirical correlations related to heat pipe are also discussed. The instruments used in the setup are seen to be accurate from their calibration graphs. Parameters like effective thermal conductivity and condenser heat transfer coefficient can be determined from this study. The results can hence be validated and the percentage deviation between results from experimental and empirical formulas can be measured. The performance of heat pipe working on nanofluid can also be studied.

Chapter 4

Results and Discussion

The results obtained from the experiments are presented in this chapter and the reasons leading to the results are also discussed. As the evaporator gains heat initially, its temperature is the higher compared to adiabatic or condenser region. The difference in average temperature of evaporator section and condenser section in a heat pipe is referred to as temperature gradient or difference. These average temperatures for each section can be computed by taking the mean value of the temperatures that are detected by the PT100 RTD sensors over that section. The average sectional temperatures as well as the temperature gradient showed a linear rise with increase in heat input on evaporator.

4.1 Effective thermal conductivity using experimental method

On increasing the heat input at the evaporator section from 40 W to 100 W, the experimental values of effective thermal conductivity increased from 32786 W/m-K to 61475 W/m-K as shown in Table 4.1.

Table 4.1: Experimental thermal conductivity data

Heat Input (Watt)	**Experimental k_{eff}** (W/m-K)
40	32786.70
50	40983.37
60	42154.33
70	49180.05
80	49180.05
90	55327.56
100	61475.06

4.2 Effective thermal conductivity using analytical model

The analytical model also predicted an increase in thermal conductivity of the heat pipe with increasing heat loads. It can be seen from Table 4.2 that the values predicted by analytical model were higher than that of experimental results but the deviations between them kept on decreasing with increase in heat input loads.

Table 4.2: Analytical thermal conductivity data

Heat Input (Watt)	**Analytical model k_{eff}** (W/m-K)
40	46764.91
50	48528.32
60	52753.43
70	54524.32
80	59656.10
90	61555.73
100	66014.01

Thermal conductivity, in general terms, is a measure of the ability of a body to allow the heat to pass through it. The thermal conductivity of metals shows a decrease with an increase in heat supply. It is because high molecular vibrations act as a restriction to the flow of free electrons in case of metals. But in heat pipes, the transfer of heat takes place through the working fluid. For liquids, the kinetic energy of their molecules is a function of temperature, so their thermal conductivity is directly proportional to heat input. So an increase was seen in the thermal conductivity values from both experimental and analytical methods with increase in heat loads. Despite the deviations between them, the graphical nature of experimental and analytical model is similar which indicates that the results are in agreement.

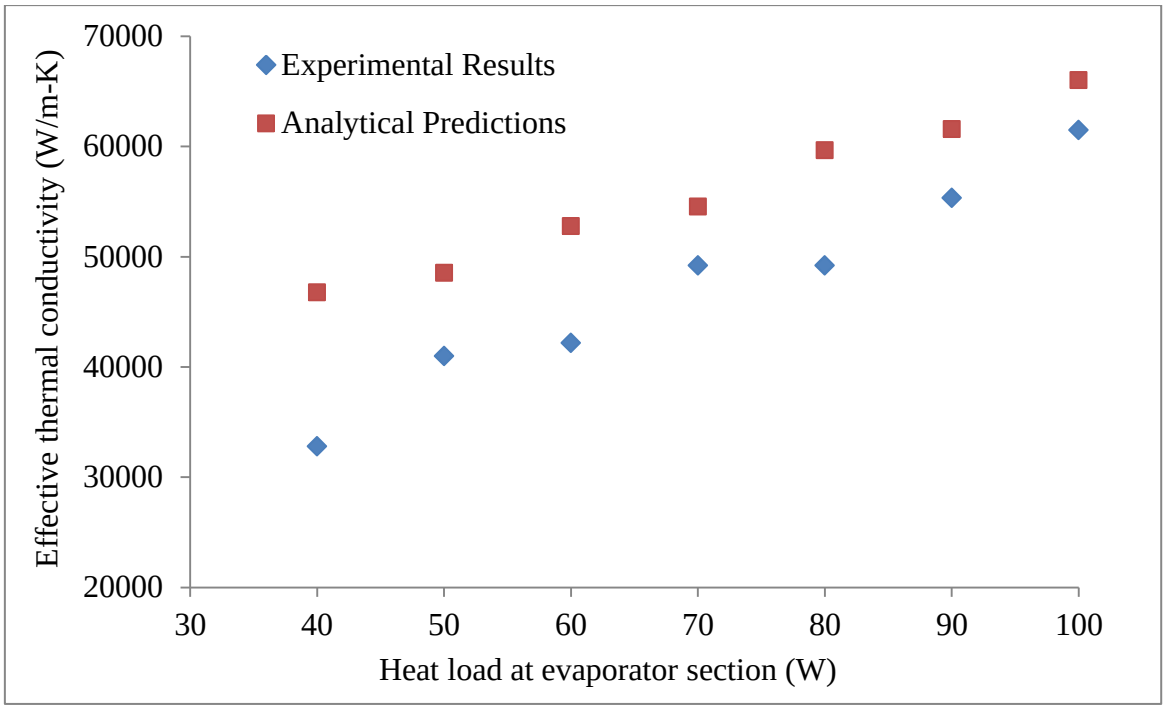

Figure 4.1: Comparison between experimental and analytical k_{eff}

A graphical comparison between results from Table 4.1 and Table 4.2 is presented in Figure 4.1. The x-axis represents heat input in Watt while the y-axis represents effective thermal conductivity of heat pipe in W/m-K. In terms of percentage, the difference between analytical and experimental values starting from lowest heat input to highest is 29.89%, 15.54%, 20.09%, 9.80%, 17.56%, 10.11% and 6.87%.

The deviations could arise be because of the fact that out of five transport limitations, only the most significant limit – the capillary limit was considered in developing the theoretical model for effective thermal conductivity of heat pipe. The uncertainties and inaccuracies present in various experimental instruments used in the test rig also account for the deviations.

Corresponding to all heat inputs, the effective thermal conductivity predicted by analytical model was higher compared to the experimental results, which was also observed by Solomon et al. [44]. The maximum deviation of 13978.21 W/m-K was observed at 40 W heat load while the minimum deviation was as low as 4538.95 W/m-K at 100 W heat load. The deviation was reduced at higher heat loads because the analytical model is based on capillary limit of heat pipe only and at higher heat inputs, capillary limit is responsible for majority of heat transfer. By using viscous, boiling, entrainment and sonic limits into consideration, we can reduce the deviations between experimental and analytical results at lower heat inputs.

4.3 Lumped resistance network approach

Using the heat pipe dimensions, material thermal properties and some wick parameters, the resistance components were determined as shown in Table 4.3, based on which the effective thermal conductivity was found to be 34292.90 W/m-K. The effect of different heat loads is not considered in these calculations because they mainly depend on material properties of heat pipe and the axial component of thermal resistance inside the heat pipe is extremely low.

Table 4.3: Lumped resistance model data

Component	Resistance
R_{pe}	7.31×10^{-8} K/W
R_{we}	1.71×10^{-6} K/W
R_{v}	5.52×10^{-8} K/W
R_{wc}	1.58×10^{-6} K/W
R_{pc}	6.75×10^{-8} K/W
R_{total}	3.42×10^{-6} K/W

4.4 Thermal resistance at different inclinations of heat pipe

The thermal resistance, which showed a linear decrease with heat loads, was obtained by taking the ratio of temperature gradient to the heat input on evaporator section. Corresponding to 10 different tilt angles of heat pipe (0˚, 5˚, 10˚, 15˚, 20˚, 25˚, 30˚, 35˚, 40˚ and 45˚) seven different heat loads were applied over the evaporator section (40 W, 50 W, 60 W, 70 W, 80 W, 90 W and 100 W). So a set of 70 experiments were performed to determine the heat pipe tilt and the heat load that offers the best results in the form of least thermal resistance to the flow of heat through the heat pipe. Graphical results for the same are demonstrated in Figure 4.2. The minimum resistance of 0.033 ˚C/W was observed at 90 W for 25˚ tilt angle. On average, the highest thermal resistance of 0.069 ˚C/W was seen at vertical 45˚ heat pipe tilt while the lowest of 0.045 ˚C/W was observed at 25 ˚ tilt. Similar results were reported by some other researchers too which proved that 15˚ to 30˚ is the best inclination range for the heat pipe [52-54]. This result could be due to the dominant gravitational forces acting in the downward direction on the condensate, thus interfering with the path of vapour flow causing evaporator flooding. In some cases, entrainment of the condensed liquid while moving through wick by the high velocity vapours also results in deteriorated performance, especially in nanofluid operated heat pipes. The graphical comparison of heat pipe thermal resistance corresponding to different tilt angles and heat loads can be as seen in Figure 4.2.

Table 4.4: Thermal resistance (˚C/W) of heat pipe at different heat loads and tilt angles

Parameter	**40 W**	**50 W**	**60 W**	**70 W**	**80 W**	**90 W**	**100 W**
0˚ tilt	0.075	0.060	0.058	0.050	0.050	0.044	0.040
5˚ tilt	0.075	0.060	0.066	0.057	0.050	0.044	0.040
10˚ tilt	0.087	0.070	0.058	0.057	0.050	0.044	0.040
15˚ tilt	0.100	0.080	0.066	0.050	0.056	0.044	0.045
20˚ tilt	0.087	0.070	0.058	0.050	0.050	0.044	0.040
25˚ tilt	0.062	0.050	0.050	0.042	0.037	0.033	0.040
30˚ tilt	0.075	0.060	0.058	0.050	0.043	0.044	0.040
35˚ tilt	0.100	0.080	0.066	0.057	0.056	0.044	0.045
40˚ tilt	0.100	0.080	0.066	0.064	0.056	0.050	0.050
45˚ tilt	0.100	0.080	0.075	0.064	0.056	0.055	0.055

Heat pipe of different types, specifications, dimensions and materials will produce different thermal resistance results. There is no particular inclination angle that can be considered valid and reliable for all heat pipes. Working fluid also plays a major role in deciding its performance as discussed in Chapter 2. The results shown in this section are for a 180 mm long copper heat pipe with 7.8 mm diameter. It is not advisable to operate copper-water heat pipe beyond 45˚ tilt angle because it showed deteriorated performance due to condenser dry-out.

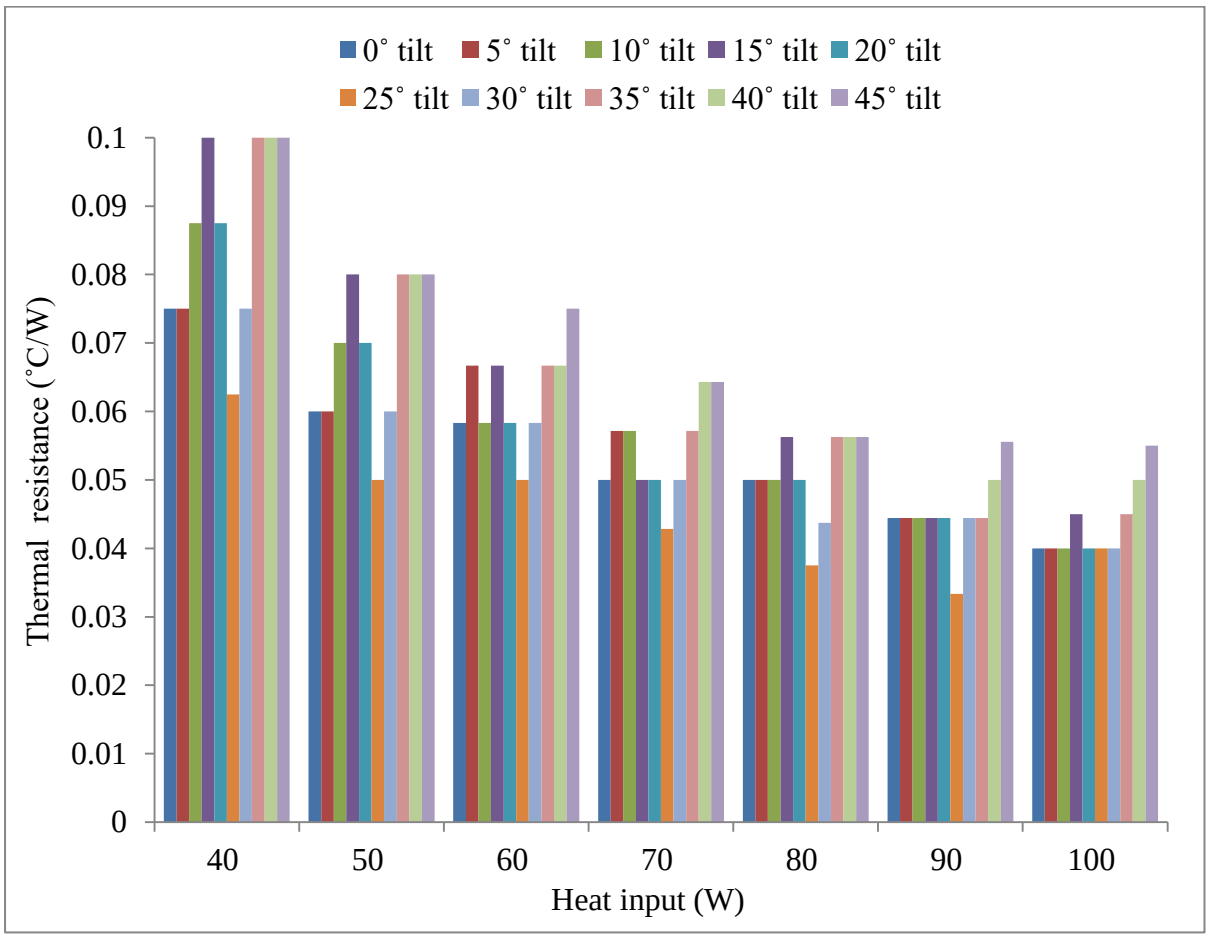

Figure 4.2: Variation of average thermal resistance w.r.t. tilt angles and heat loads

4.5 Thermal resistance with and without Al_2O_3 nanoparticles

Two heat pipes were used in this study and the experimentation was done at 0˚ horizontal position of heat pipes only. For both the heat pipes, i.e. with and without Al_2O_3 nanoparticles, the thermal resistance decreased with increase in heat input. It can be seen from Figure 4.3 that the thermal resistance in case of heat pipe with nanoparticles is less than (or equal to in some cases) that of heat pipe that only has water as its working fluid. The minimum thermal resistance of 0.033 ˚C/W was observed corresponding to 90 W heat load on the evaporator

section of alumina nanoparticle operated heat pipe. Also the maximum resistance to the flow of heat for the same heat pipe was significantly lesser at 0.0625 ˚C/W compared to water heat pipe at 0.075 ˚C/W when the heat input was 40 W.

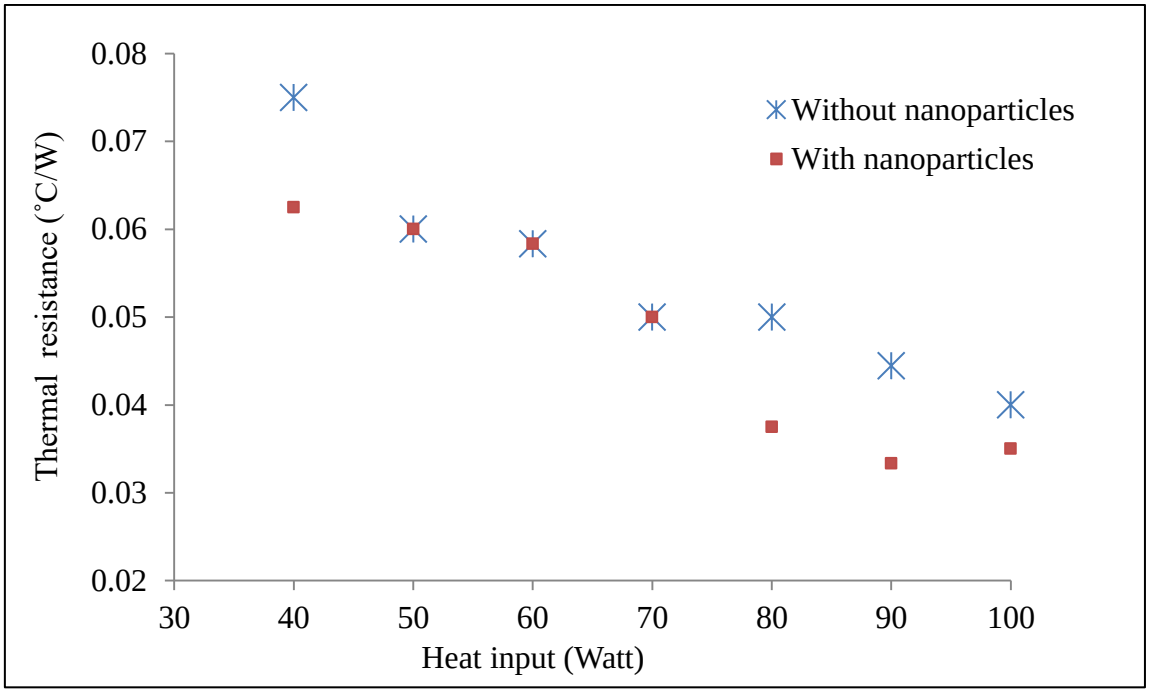

Figure 4.3: Comparison of heat pipe thermal resistance with and without nanoparticles

The thermal resistance in this study was determined based on the average surface temperatures over evaporator and condenser sections. For both heat pipes, the resistance offered to the flow of heat is high at low input loads but it decreases as the input load is increased. The operating range of heat pipe increases due to addition of nanoparticles, hence dry-out occurs at higher temperatures, which is a major advantage. Also the addition of nanoparticles increases the thermal conductivity and surface area of wick [44], resulting in reduced thermal resistance. Pure water heat pipe has more thermal resistance because there is a huge bubble nucleation size in evaporator section compared to Al_2O_3 heat pipe [55]. The addition of nanoparticles also decreases the contact angle inside the heat pipe, hence increasing surface wettability and capillary pumping capacity [56].

4.6 Condenser heat transfer coefficients at different heat loads

The heat transfer coefficient on the external surface of the condenser section in case of free convection was determined using Eq. (3.23) and compared to the experimental heat transfer

coefficient for every different heat load. The nature of plots in both the cases was similar as seen in Figure 4.4 even though the deviation between experimental and predicted values of 23.35%, 22.49%, 19.48%, 21.28%, 21.70%, 23.59% and 24.58% was seen. Practically, natural or free convection is very hard to achieve and the real surfaces are generally isothermal, therefore we always get variations between these results. The deviations are permissible because calculated values can vary ±25% from what is experienced in experiments [51]. Similar values of heat transfer coefficient in range of 11.5 W/m^{2}K to 13.1 W/m^{2}K (predicted) and 9.7 W/m^{2}K to 11.8 W/m^{2}K (experimental) were also attained by Kumar and Gangacharyulu [25].

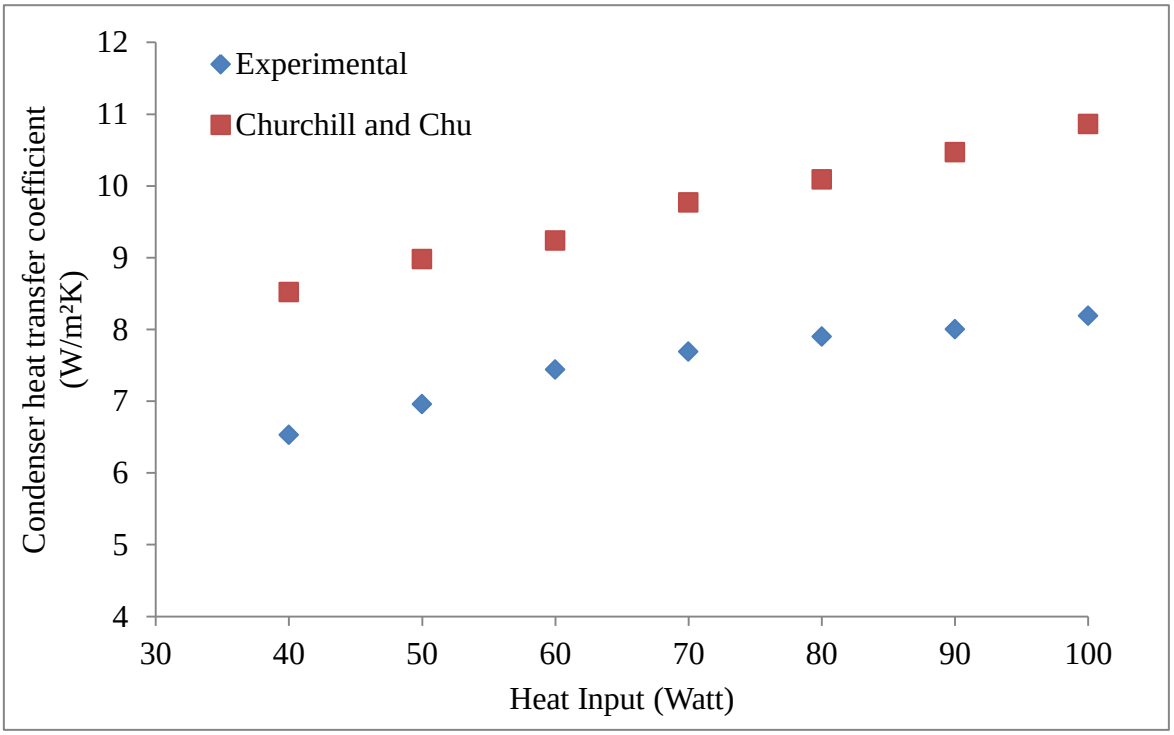

Figure 4.4: Predicted and experimental heat transfer coefficients in free convection

The values of heat transfer coefficient over condenser section were more in case of forced convection compared to that of natural convection. Heat transfer coefficient is directly proportional to the rate at which transfer of heat takes place. The reason for higher heat transfer coefficient in forced convection is because in this case, hot air surrounding the condenser section is immediately removed by the flow of air around it. Nusselt number is proportional to Reynolds number. And Reynolds number is proportional to the fluid flow velocity. We know that in case of forced convection, the velocity of air is more than that of free convection. So, the magnitude of Nusselt number and the corresponding heat transfer

coefficient increases. The graphical comparison among forced convective heat transfer coefficients for experimental results and that of different empirical correlations can be seen in Figure 4.5.

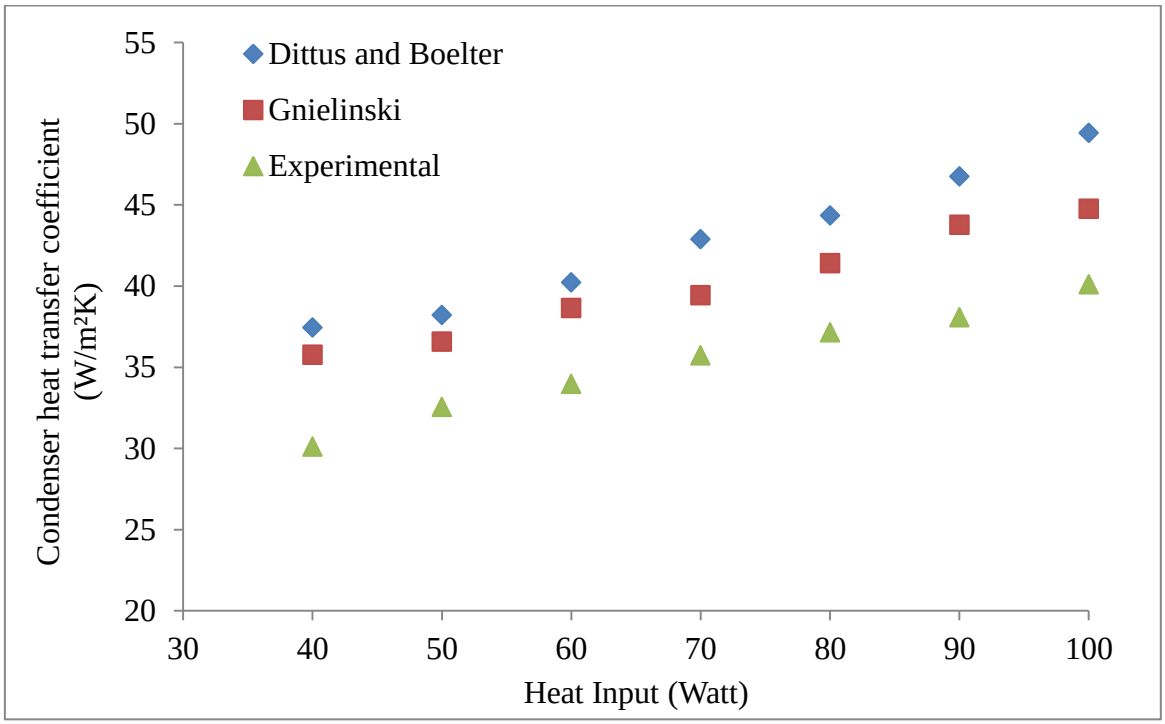

Figure 4.5: Comparison of condenser heat transfer coefficients in forced convection

In terms of percentage, deviations of 24.34%, 17.38%, 18.36%, 19.97%, 19.35%, 22.79% and 23.29% corresponding to 7 different heat inputs starting from 40 W to 100 W were observed between experimental results and empirical predictions from Dittus and Boelter's correlation. As seen from Figure 4.5, the variations between empirical results from Gnielinski's correlation and experiments were significantly less compared to the previous case with changes of 15.82%, 10.98%, 12.06%, 9.38%, 10.26%, 12.90% and 10.43%. All these deviations were within permissible limits [51].

4.7 Summary

Faghri's analytical model based on capillary limit was accurate in predicting the effective thermal conductivity of the heat pipe. Even though significant deviations between experiments and analytical calculations were observed at lower heat inputs, but the results at higher heat inputs were seen to be in agreement because capillary forces play a major role at high temperatures. A lumped model of thermal resistance is also used to find the thermal

resistance and thermal conductivity of heat pipe based on the internal properties and dimensions of the pipe. Addition of nanofluids in the base water working fluid can improve the performance of a heat pipe by increasing its effective thermal conductivity and by reducing its thermal resistance. However, sedimentation of nanoparticles in the wick structure is a major problem in heat pipes that can ultimately affect their performance in the long run. Gnielinski's correlation was found to be more accurate in predicting the values of heat transfer coefficient compared to Dittus and Boelter correlation. It is a more complex correlation as it incorporates the friction factor, but it is valid for a wide range of Reynolds number. Gnielinski's correlation is also applicable in transition region.

Chapter 5

Conclusions and Future Scope

5.1 Conclusions

In this chapter, the conclusions drawn from the results are presented. Various experiments were performed on a copper-water heat pipe to check its performance under different conditions. The following interpretations can be made from the study conducted in this thesis work.

1. With the increase in Evaporator heat load, thermal conductivities predicted by Faghri's model as well as by experiments showed an increase. The nature of their increase as studied from the graphical comparison is in fair agreement.

2. As the heat load is increased, the deviation between Analytical result and Experimental result for effective thermal conductivity gets smaller. Highest deviation was at 29.89% at 40 W heat load while minimum deviation was 6.87% at 100 W.

3. The resistance offered to the flow of heat while travelling from evaporator to condenser section axially is low compared to the resistances offered by heat pipe wall and wick structure as the condition within the cylinder is that of vacuum.

4. The effective thermal conductivity of the heat pipe using lumped resistance network analysis was found to be 34292.90 W/m-K after neglecting the axial thermal resistance inside the heat pipe.

5. While performing experiments from 40 W to 100 W, the lowest temperature differential between evaporator and condenser ends was recorded as 2.5 ˚C and highest as 5.5 ˚C which reflects on the efficient performance of heat pipe with minimum heat loss.

6. The lowest value of thermal resistance for copper-water heat pipe came out to be 0.033˚C/W, which was seen at 25˚ inclination angle of the pipe, when the heat load on the

evaporator end was 90 W. Overall, the best performance was observed at 25˚ tilt and comparatively poor performance was observed above the angles of 40 ˚.

7. The average thermal resistance over all heat input experiments was highest at 45˚ tilt with 0.069 ˚C/W, so it is not recommended to use copper-water heat pipe at large tilt angles. Thermal resistance was very high corresponding to 40 W heat load when the tilt angles were greater than 30˚.

8. Heat pipe with aluminum oxide nanoparticles (Al_2O_3)/water working fluid offered lesser thermal resistance compared to copper-water heat pipe at heat loads of 40 W, 80 W, 90 and 100 W. But corresponding to heat loads of 50 W, 60 W and 70 W, the thermal resistance of both the heat pipes was same.

9. For free as well as forced convection, the heat transfer coefficient over condenser section showed a gradual rise with increase in heat input on the evaporator section. The predicted and experimental results were in good agreement with deviations no more than 25%.

10. Significant enhancement was observed in heat transfer coefficient by using forced convection over condenser surface. The maximum heat transfer coefficient under natural convection was 8.19 W/m^2K but in case of forced convection, it was 40.10 W/m^2K.

5.2 Future Scope

Heat Pipe technology is being employed in a lot of industries these days. Despite a wide range of experimental work in this field, some scope for future work was realised after concluding the thesis. Further research work could be done in future on the following points:

1. The heat input to the evaporator section of the heat pipe could be done by using different fluids depending on the application for which the heat pipe is employed.

2. Settlement of working fluid particles when the heat pipe is not in use for some days, especially in the case of nanofluids, is a major problem in the heat pipes, which deteriorates the performance. The precautionary measures to be taken regarding standby time of heat pipe operating on different working fluids should be established.

3. The design and specification of fins for different types of heat pipes could be improved to enhance heat removal from condenser section. The resistance between fin and heat pipe surface could be minimized by certain coatings or other soldering techniques without causing any damage to the heat pipe surface.

4. Research could be done on the performance of the heat pipe by varying the lengths of evaporator, adiabatic and condenser section and hence establishing a relation for maximum and minimum length ratio for each section.

References

1. Perkins, J., 1836. UK Patent No. 7059.

2. Gaugler, R., 1944, "Heat Transfer Device," U.S. Patent No. 2350348.

3. Grover, G.M., 1966. Evaporation-condensation heat transfer device. U.S. Patent 3,229,759.

4. Dunn, P.D. and Reay, D., 2012. Heat pipes. Elsevier.

5. Vasiliev, L.L., 2005. Heat pipes in modern heat exchangers. Applied thermal Engg, 25(1), pp.1-19.

6. Faghri, A., 2014. Heat pipes: review, opportunities and challenges. Frontiers in Heat Pipes (FHP), 5(1).

7. Khalkhali, H., Faghri, A. and Zuo, Z.J., 1999. Entropy generation in a heat pipe system. Applied Thermal Engineering, 19(10), pp.1027-1043.

8. Chen, M.M. and Morgan, M., 1989. Heat transfer characteristics in two-phase closed conventional and concentric annular thermosyphons.

9. Mochizuki, M., Saito, Y., Kiyooka, F. and Nguyen, T., 2006, September. High Power Cooling Chips by Heat Pipes and Advanced Heat Spreader. In 8th International Heat Pipe Symposium, Kumamoto, Japan (pp. 214-221).

10. Wu, X.P., Mochizuki, M., Mashiko, K., Nguyen, T., Nguyen, T., Wuttijumnong, V., Cabusao, G., Singh, R. and Akbarzadeh, A., 2011. Cold energy storage systems using heat pipe technology for cooling data centers. Frontiers in Heat Pipes (FHP), 2(1).

11. Jalilvand, A., Katsuta, M., Saito, K., Toyonaga, J. and Mochizuki, M., 2006. The Study On The Thermal Performance Of Concentric Annular Heat Pipe With The Application In The Heat Roll Of Fusing Unit Of Copy Machine. In International Heat Transfer Conference 13. Begel House Inc.

12. Trefethen, L., 1962. On the surface tension pumping of liquids or a possible role of the candlewick in space exploration. Tech Info., GE, Serial, (615), p.D114.

13. Zhang, H. and Zhuang, J., 2003. Research, development and industrial application of heat pipe technology in China. Applied Thermal Engineering, 23(9), pp.1067-1083.

14. Loh, C.K., Harris, E. and Chou, D.J., 2005, March. Comparative study of heat pipes performances in different orientations. In Semiconductor Thermal Measurement and Management Symposium, 2005 IEEE Twenty First Annual IEEE (pp. 191-195). IEEE.

15. Kang, S.W., Wei, W.C., Tsai, S.H. and Yang, S.Y., 2006. Experimental investigation of silver nano-fluid on heat pipe thermal performance. Applied Thermal Engineering, 26(17), pp.2377-2382.

16. Noie, S.H., Sarmasti Emami, M.R. and Khoshnoodi, M., 2007. Effect of inclination angle and filling ratio on thermal performance of a two-phase closed thermosyphon under normal operating conditions. Heat transfer engineering, 28(4), pp.365-371.

17. Meena, P., Rittidech, S. and Tammasaeng, P., 2008. Effect of inner diameter and inclination angles on operation limit of closed-loop oscillating heat-pipes with check valves. American Journal of Engineering and Applied Sciences, 1(2).

18. Hudakorn, T., Terdtoon, P. and Sakulchangsatjatai, P., 2008. Effect of inclination angle on performance limit of a closed-end oscillating heat pipe. American Journal of Engineering and Applied Sciences, 1(3), pp.174-180.

19. Huminic, G. and Huminic, A., 2009, July. CFD Study of the heat pipes with water–nanoparticles mixture. In Proceeding of European Automotive Simulation Conference, EASC (Vol. 2009, pp. 217-228).

20. Grooten, M.H.M. and Van Der Geld, C.W.M., 2010. The effect of the angle of inclination on the operation limiting heat flux of long R-134a filled thermosyphons. Journal of heat transfer, 132(5), p.051501.

21. Teng, Tun-Ping, How-Gao Hsu, Huai-En Mo, and Chien-Chih Chen. "Thermal efficiency of heat pipe with alumina nanofluid." Journal of Alloys and Compounds 504 (2010): S380-S384.

22. Riehl, R.R. and dos Santos, N., 2012. Water-copper nanofluid application in an open loop pulsating heat pipe. Applied Thermal Engineering, 42, pp.6-10.

23. Mousa, M.G., 2011. Effect of nanofluid concentration on the performance of circular heat pipe. Ain shams engineering journal, 2(1), pp.63-69.

24. Senthilkumar, R., Vaidyanathan, S. and Sivaraman, B., 2011. Performance investigation of heat pipe using aqueous solution of n-Pentanol with different inclinations. Journal of mechanical science and technology, 25(4), pp.923-929.

25. Vikas Kumar , D. Gangacharyulu & Ram Gopal Tathgir (2007) Heat Transfer Studies of a Heat Pipe, Heat Transfer Engineering, 28:11, 954-965.

26. Solomon, A. Brusly, K. Ramachandran, and B. C. Pillai. "Thermal performance of a heat pipe with nanoparticles coated wick." Applied Thermal Engineering 36 (2012): 106-112.

27. Moraveji, Mostafa Keshavarz, and Sina Razvarz. "Experimental investigation of aluminum oxide nanofluid on heat pipe thermal performance."International Communications in Heat and Mass Transfer 39, no. 9 (2012): 1444-1448.

28. Manimaran, R., Palaniradja, K., Alagumurthi, N. and Hussain, J., 2012. Factors affecting the thermal performance of heat pipe–a review. Journal of Engineering Research and Studies, 3(2), pp.20-24.

29. Pachghare, P.R. and Mahalle, A.M., 2013, July. Effect of Inclination Angle on the Closed Loop Pulsating Heat Pipe Thermal Performance. In ASME 2013 Heat Transfer Summer Conference collocated with the ASME 2013 7th International Conference on Energy Sustainability and the ASME 2013 11th International Conference on Fuel Cell Science, Engineering and Technology (pp. V002T07A027-V002T07A027). American Society of Mechanical Engineers.

30. Hung, Yi-Hsuan, Tun-Ping Teng, and Bo-Gu Lin. "Evaluation of the thermal performance of a heat pipe using alumina nanofluids." Experimental Thermal and Fluid Science 44 (2013): 504-511.

31. Peyghambarzadeh, S.M., Shahpouri, S., Aslanzadeh, N. and Rahimnejad, M., 2013. Thermal performance of different working fluids in a dual diameter circular heat pipe. Ain Shams Engineering Journal, 4(4), pp.855-861.

32. Xue, Z. and Qu, W., 2014. Experimental study on effect of inclination angles to ammonia pulsating heat pipe. Chinese Journal of Aeronautics, 27(5), pp.1122-1127.

33. Idrus, F., Mohamad, N., Zailani, R., Wisnoe, W. and Abdullah, M.Z., 2014. Thermal Performance of a Cylindrical Heat Pipe for Different Heat Inputs and Inclination Angles. In Applied Mechanics and Materials (Vol. 661, pp. 148-153). Trans Tech Publications.

34. Kumar, R. Reji, K. Sridhar, and M. Narasimha. "Heat Transfer Performance in Heat Pipe Using Al_2O_3-DI Water Nanofluid." International Journal of Material and Mechanical Engineering 3, no. 1 (2014): 1-5.

35. Yang, C., Chang, C., Song, C., Shang, W., Wu, J., Tao, P. and Deng, T., 2016. Fabrication and performance evaluation of flexible heat pipes for potential thermal control of foldable electronics. Applied Thermal Engineering, 95, pp.445-453.

36. Nazarimanesh, M., Yousefi, T. and Ashjaee, M., 2015. Experimental study on the effects of inclination situation of the sintered heat pipe on its thermal performance. Experimental Thermal and Fluid Science, 68, pp.625-633.

37. Hassan, Mohamed I., Pawan K. Singh, Waka Tesfai, and Youssef Shatilla. "An experimental study of heat pipe performance using nanofluids."International Journal of Green Energy 12, no. 3 (2015): 225-229.

38. Nookaraju, B.C., Rao, P.K. and Nagasarada, S., 2015. Experimental and Numerical Analysis of Thermal Performance in Heat Pipes. Procedia Engineering, 127, pp.800-808.

39. Hassan, Mohamed I., Ismail A. Alzarooni, and Youssef Shatilla. "The Effect of Water-Based Nanofluid Incorporating Al_2O_3 Nanoparticles on Heat Pipe Performance." Energy Procedia 75 (2015): 3201-3206.

40. Ghanbarpour, M., Nikkam, N., Khodabandeh, R., Toprak, M.S. and Muhammed, M.Thermal performance of screen mesh heat pipe with Al_2O_3nanofluid. Experimental Thermal and Fluid Science, 66, 2015: pp.213-220.

41. Chen, J.S. and Chou, J.H., 2015. Thermal Performance of Cooling Enhancement of Miniature Flat Plate Heat Pipe Under Different Angle. Journal of Mechanics, pp.1-8.

42. Hussain, M.N. and Janajreh, I., 2016. Numerical Simulation of a Cylindrical Heat Pipe and Performance Study. Int. J. of Thermal & Environmental Engineering, 12(2), pp.135-141.

43. Remeli, M.F., Date, A., Orr, B., Ding, L.C., Singh, B., Affandi, N.D.N. and Akbarzadeh, A., 2016. Experimental investigation of combined heat recovery and power generation using a heat pipe assisted thermoelectric generator system. Energy Conversion and Management, 111, pp.147-157.

44. Solomon, A.B., Sekar, M. and Yang, S.H., 2016. Analytical expression for thermal conductivity of heat pipe. Applied Thermal Engineering, 100, pp.462-467.

45. Bhullar, B.S., Gangacharyulu, D. and Das, S.K., 2017. Temporal deterioration in thermal performance of screen mesh wick straight heat pipe using surfactant free aqueous nanofluids. Heat and Mass Transfer, 53(1), pp.241-251.

46. Cong, L., Qifei, J. and Wu, S., 2016. Experimental and theoretical analysis on the effect of inclination on metal powder sintered heat pipe radiator with natural convection cooling. Heat and Mass Transfer, pp.1-9.

47. Hong, S., Wang, S. and Zhang, Z., 2016. Multiple orientations research on heat transfer performances of Ultra-Thin Loop Heat Pipes with different evaporator structures. International Journal of Heat and Mass Transfer, 98, pp.415-425.

48. Goshayeshi, H.R., Safaei, M.R., Goodarzi, M. and Dahari, M., 2016. Particle size and type effects on heat transfer enhancement of Ferro-nanofluids in a pulsating heat pipe. Powder Technology, 301, pp.1218-1226.

49. Chi, S.W., 1976. Heat pipe theory and practice: a sourcebook.

50. Chapman, A.J., Fundamentals of Heat Transfer, 1987.

51. Holman, J.P., 2010. Heat transfer. McGraw-hill.

52. Tathgir, R.G., Kumar, A. and Gangacharyulu, D., 1999. Performance Characterstics of a Carbon Steel Heat Pipe at Low Temperature Range. In Proceedings of the 11th Intl. Heat Pipe Conference (Vol. 2). Musashinoshi, Tokyo, Japan.

53. Negishi, K., Kaneko, K., Matsuoka, T., Hirashima, M., Nishikawa, Y. and Taguchi, M., 1991. Heat-transfer performance of a corrugated-tube thermosiphon. Part 1; Evaporator performance. Heat Transfer-Japanese Research;(United States), 20(2).

54. Abhat, A. and Nguyenchi, H., 1976. Investigation of performance of gravity assisted copper-water heat pipes. Heat Pipes.

55. Moraveji, M.K. and Razvarz, S., 2012. Experimental investigation of aluminum oxide nanofluid on heat pipe thermal performance. International Communications in Heat and Mass Transfer, 39(9), pp.1444-1448.

56. Asirvatham, L.G., Nimmagadda, R. and Wongwises, S., 2013. Heat transfer performance of screen mesh wick heat pipes using silver–water nanofluid. International Journal of Heat and Mass Transfer, 60, pp.201-209.

Annexure

Table A1: Calibration data of rotameter (all readings in ml/min)

Flow Rate	Test 1	Test 2	Test 3	Test 4	Test 5
25	26	26	25	26	25
50	52	51	50	52	50
75	77	77	76	76	76
100	101	103	101	101	102
125	128	128	127	128	129
150	155	155	154	154	153

Table A2: Calibration data of temperature sensors on water heat pipe (all readings in ˚C)

Thermometer Readings	TS-1	TS-2	TS-3	TS-4	TS-5	TS-6
25	26	26	25	24	25	26
30	29	29	30	31	29	31
35	34	35	35	35	34	35
40	39	41	40	40	40	39
45	45	44	46	44	45	44
50	51	51	49	50	50	50
55	55	56	55	55	55	56
60	61	60	60	61	60	61

Table A3: Calibration data of temperature sensors on water-nanofluid heat pipe (˚C)

Thermometer Readings	**TS-1**	**TS-2**	**TS-3**	**TS-4**	**TS-5**	**TS-6**
25	26	25	25	24	26	26
30	31	31	29	30	29	29
35	34	34	34	35	35	34
40	40	40	41	41	40	41
45	46	45	44	44	45	44
50	50	51	50	50	50	51
55	56	56	56	54	55	55
60	61	61	59	58	58	60

Table A4: Thermo-physical properties of air at different film temperatures

Film Temperature, T_f (^oC)	**Volumetric Expansion Coefficient, β** (1/K)	**Kinematic Viscosity, ν** (m^2/s)	**Thermal Conductivity, k** (W/m-K)	**Prandtl Number, Pr**
33.75	3.2584×10^{-3}	1.6389×10^{-5}	0.026618	0.71311
34.75	3.2478×10^{-3}	1.6483×10^{-5}	0.026691	0.71294
36.25	3.2321×10^{-3}	1.6625×10^{-5}	0.026801	0.71268
37.25	3.2216×10^{-3}	1.6720×10^{-5}	0.026875	0.71252
38.25	3.2113×10^{-3}	1.6815×10^{-5}	0.026948	0.71235
38.75	3.2062×10^{-3}	1.6862×10^{-5}	0.026985	0.71227
39.75	3.1959×10^{-3}	1.6958×10^{-5}	0.027058	0.71211

Table A5: Thermal resistance data at 0° heat pipe inclination

Heat Input (Watt)	**TS-1** (˚C)	**TS-2** (˚C)	**TS-3** (˚C)	**TS-4** (˚C)	**TS-5** (˚C)	**TS-6** (˚C)	**T_{in}** (˚C)	**T_{out}** (˚C)	**ΔT** (˚C)	**R** (˚C/W)
40	39	38	34	34	36	35	38.5	35.5	3	0.075
50	41	40	37	36	38	37	40.5	37.5	3	0.06
60	44	44	39	39	41	40	44	40.5	3.5	0.058333
70	46	46	40	40	43	42	46	42.5	3.5	0.05
80	49	48	43	42	45	44	48.5	44.5	4	0.05
90	50	49	44	43	46	45	49.5	45.5	4	0.044444
100	52	51	46	45	48	47	51.5	47.5	4	0.04

Table A6: Thermal resistance data at 5° heat pipe inclination

Heat Input (Watt)	**TS-1** (˚C)	**TS-2** (˚C)	**TS-3** (˚C)	**TS-4** (˚C)	**TS-5** (˚C)	**TS-6** (˚C)	**T_{in}** (˚C)	**T_{out}** (˚C)	**ΔT** (˚C)	**R** (˚C/W)
40	39	38	34	34	36	35	38.5	35.5	3	0.075
50	41	40	37	36	38	37	40.5	37.5	3	0.06
60	44	44	39	39	40	40	44	40	4	0.066667
70	46	46	40	40	42	42	46	42	4	0.057143
80	49	48	43	42	45	44	48.5	44.5	4	0.05
90	50	49	44	43	46	45	49.5	45.5	4	0.044444
100	52	51	46	45	48	47	51.5	47.5	4	0.04

Table A7: Thermal resistance data at 10° heat pipe inclination

Heat Input (Watt)	**TS-1** (˚C)	**TS-2** (˚C)	**TS-3** (˚C)	**TS-4** (˚C)	**TS-5** (˚C)	**TS-6** (˚C)	**T_{in}** (˚C)	**T_{out}** (˚C)	**ΔT** (˚C)	**R** (˚C/W)
40	40	38	34	34	36	35	39	35.5	3.5	0.0875
50	42	40	37	36	38	37	41	37.5	3.5	0.07
60	44	44	39	39	41	40	44	40.5	3.5	0.058333
70	46	46	40	40	42	42	46	42	4	0.057143
80	49	48	43	42	45	44	48.5	44.5	4	0.05
90	50	49	44	43	46	45	49.5	45.5	4	0.044444
100	52	51	46	45	48	47	51.5	47.5	4	0.04

Table A8: Thermal resistance data at 15° heat pipe inclination

Heat Input (Watt)	**TS-1** (˚C)	**TS-2** (˚C)	**TS-3** (˚C)	**TS-4** (˚C)	**TS-5** (˚C)	**TS-6** (˚C)	**T_{in}** (˚C)	**T_{out}** (˚C)	**ΔT** (˚C)	**R** (˚C/W)
40	40	39	34	34	36	35	39.5	35.5	4	0.1
50	42	40	37	36	37	37	41	37	4	0.08
60	44	44	39	39	40	40	44	40	4	0.066667
70	46	46	40	40	43	42	46	42.5	3.5	0.05
80	49	48	43	42	44	44	48.5	44	4.5	0.05625
90	50	49	44	43	46	45	49.5	45.5	4	0.044444
100	52	52	46	45	48	47	52	47.5	4.5	0.045

Table A9: Thermal resistance data at 20° heat pipe inclination

Heat Input (Watt)	**TS-1** (˚C)	**TS-2** (˚C)	**TS-3** (˚C)	**TS-4** (˚C)	**TS-5** (˚C)	**TS-6** (˚C)	**T_{in}** (˚C)	**T_{out}** (˚C)	**ΔT** (˚C)	**R** (˚C/W)
40	40	39	34	34	36	36	39.5	36	3.5	0.0875
50	42	40	37	36	38	37	41	37.5	3.5	0.07
60	44	44	39	39	41	40	44	40.5	3.5	0.058333
70	46	46	40	40	43	42	46	42.5	3.5	0.05
80	49	48	43	42	45	44	48.5	44.5	4	0.05
90	50	49	44	43	46	45	49.5	45.5	4	0.044444
100	52	52	46	45	48	48	52	48	4	0.04

Table A10: Thermal resistance data at 25° heat pipe inclination

Heat Input (Watt)	**TS-1** (˚C)	**TS-2** (˚C)	**TS-3** (˚C)	**TS-4** (˚C)	**TS-5** (˚C)	**TS-6** (˚C)	**T_{in}** (˚C)	**T_{out}** (˚C)	**ΔT** (˚C)	**R** (˚C/W)
40	40	39	34	34	37	37	39.5	37	2.5	0.0625
50	42	40	37	36	39	38	41	38.5	2.5	0.05
60	44	44	39	39	41	41	44	41	3	0.05
70	46	46	40	40	43	43	46	43	3	0.042857
80	49	48	43	42	46	45	48.5	45.5	3	0.0375
90	50	49	44	43	47	46	49.5	46.5	3	0.033333
100	52	52	46	45	48	48	52	48	4	0.04

Table A11: Thermal resistance data at 30° heat pipe inclination

Heat Input (Watt)	**TS-1** (˚C)	**TS-2** (˚C)	**TS-3** (˚C)	**TS-4** (˚C)	**TS-5** (˚C)	**TS-6** (˚C)	**T_{in}** (˚C)	**T_{out}** (˚C)	**ΔT** (˚C)	**R** (˚C/W)
40	40	40	34	34	37	37	40	37	3	0.075
50	42	40	37	36	38	38	41	38	3	0.06
60	44	44	39	39	41	40	44	40.5	3.5	0.058333
70	46	46	40	40	43	42	46	42.5	3.5	0.05
80	49	48	43	42	45	45	48.5	45	3.5	0.04375
90	50	49	44	43	46	45	49.5	45.5	4	0.044444
100	52	52	46	45	48	48	52	48	4	0.04

Table A12: Thermal resistance data at 35° heat pipe inclination

Heat Input (Watt)	**TS-1** (˚C)	**TS-2** (˚C)	**TS-3** (˚C)	**TS-4** (˚C)	**TS-5** (˚C)	**TS-6** (˚C)	**T_{in}** (˚C)	**T_{out}** (˚C)	**ΔT** (˚C)	**R** (˚C/W)
40	40	40	34	34	36	36	40	36	4	0.1
50	42	40	37	36	37	37	41	37	4	0.08
60	44	44	39	39	40	40	44	40	4	0.066667
70	46	46	40	40	42	42	46	42	4	0.057143
80	49	48	43	42	44	44	48.5	44	4.5	0.05625
90	50	49	44	43	46	45	49.5	45.5	4	0.044444
100	52	52	46	45	48	47	52	47.5	4.5	0.045

Table A13: Thermal resistance data at 40° heat pipe inclination

Heat Input (Watt)	**TS-1** (˚C)	**TS-2** (˚C)	**TS-3** (˚C)	**TS-4** (˚C)	**TS-5** (˚C)	**TS-6** (˚C)	**T_{in}** (˚C)	**T_{out}** (˚C)	**ΔT** (˚C)	**R** (˚C/W)
40	40	40	34	34	36	36	40	36	4	0.1
50	42	40	37	36	37	37	41	37	4	0.08
60	44	44	39	39	40	40	44	40	4	0.066667
70	46	46	40	40	42	41	46	41.5	4.5	0.064286
80	49	48	43	42	44	44	48.5	44	4.5	0.05625
90	50	49	44	43	45	45	49.5	45	4.5	0.05
100	52	52	46	45	47	47	52	47	5	0.05

Table A14: Thermal resistance data at 45° heat pipe inclination

Heat Input (Watt)	**TS-1** (˚C)	**TS-2** (˚C)	**TS-3** (˚C)	**TS-4** (˚C)	**TS-5** (˚C)	**TS-6** (˚C)	**T_{in}** (˚C)	**T_{out}** (˚C)	**ΔT** (˚C)	**R** (˚C/W)
40	40	40	34	34	36	36	40	36	4	0.1
50	42	40	37	36	37	37	41	37	4	0.08
60	44	44	39	39	41	40	44	39.5	4.5	0.075
70	46	46	40	40	42	41	46	41.5	4.5	0.064286
80	49	48	43	42	44	44	48.5	44	4.5	0.05625
90	50	50	44	43	45	45	50	45	5	0.055556
100	52	52	46	45	47	46	52	46.5	5.5	0.055